COMPUTER METHODS IN MATERIALS SCIENCE

2024, vol. 24, no. 4, 5–35
https://doi.org/10.7494/cmms.2024.4.1010

Mechanical behavior of adhesive joints: A review on modeling techniques

Maximilian Ries*

Institute of Applied Mechanics, Friedrich-Alexander-Universität Erlangen-Nürnberg, Germany.

Abstract

In the pursuit of lighter designs, many industries are shifting from conventional fasteners to adhesive joints, which offer a better strength-to-weight ratio and facilitate the use of fiber-reinforced polymers. However, modeling adhesive joints presents major challenges due to the complex behavior of polymeric adhesives and the microstructural changes induced by the substrates. As a result, various simulation methods have been developed to capture the behavior of adhesive joints across different scales. Molecular dynamics studies address atomistic and nanoscale phenomena, while continuum approaches – such as the finite element method, cohesive zone models, and peridynamics – focus on meso and macro scales. Additionally, multiscale methods combine particle and continuum approaches to provide a more comprehensive understanding of the adhesive bond behavior. This review paper offers an overview of the most relevant numerical methods employed to examine the mechanical behavior of adhesive joints and illustrates the simulations' applications through examples from the literature.

Keywords: adhesive joint, modeling techniques, mechanical behavior

1. Introduction

Lightweight design is one of the key challenges for modern engineering in achieving cost-efficiency and sustainability goals. In this context, adhesively bonded joints are a pivotal technology enabling weight reduction due to their better strength-to-weight ratio (Silva & Campilho, 2011) compared to conventional fastening methods (Pramanik et al., 2017), like riveting, welding, or bolting. Moreover, they allow the bonding of dissimilar materials, e.g., polymer composite and aluminum, without damaging them, facilitating the use of lightweight fiber-reinforced polymers (FRP) (Taib et al., 2006). Therefore, adhesive joints are increasingly employed by the automotive (Scattina et al., 2011) and aerospace industry (Soutis, 2005) but are also used for plastic integrated circuits (Jin F.-L. et al., 2015), enamel-polymer bonds in dental medicine (Cadenaro et al., 2019), or FRP reinforcement of concrete structures in civil engineering (Zhang et al., 2017). The high relevance of adhesive joints is also reflected in scientific research, as an increasing number of journal publications address this topic, cf. Figure 1a.

The modeling of adhesive joints, however, poses multiple challenges. On the one hand, there is the complex material behavior of the adhesives comprising hyperelasticity, plasticity (Mohapatra & Smith, 2019; Raghava et al., 1973), load rate-dependent (Carlberger et al., 2009; Viana et al., 2018) and temperature-dependent behavior (Jia et al., 2018; Marques et al., 2014), as well as material damage (Banea et al., 2010;

* Author's email: maximilian.ries@fau.de
ORCID ID: 0000-0002-7351-6521

Tserpes et al., 2021). On the other hand, the polymer morphology changes near the adherend, resulting in a region where curing degree (Wehlack & Possart, 2005), glass transition temperature (Häßler & Mühlen, 2000; Meiser et al., 2008), and mechanical properties (Possart G., 2014; Roche et al., 1994) deviate from the bulk adhesive (Maguire et al., 1994). This so-called *interphase* exhibits a thickness of a few nanometers up to hundreds of micrometers, depending on the investigated properties (Aufray & Roche, 2007; Meiser et al., 2010). The property changes affect the joint's overall behavior and are highly dependent on the material pairing (Passlack et al., 2009; Possart W. et al., 2006), manufacturing conditions (Fata et al., 2005), and application environment (Kanzow et al., 2005; Meiser & Possart, 2011). Consequently, the macroscopic behavior of adhesive joints is governed by the molecular microstructure, which necessitates modeling efforts at different scales.

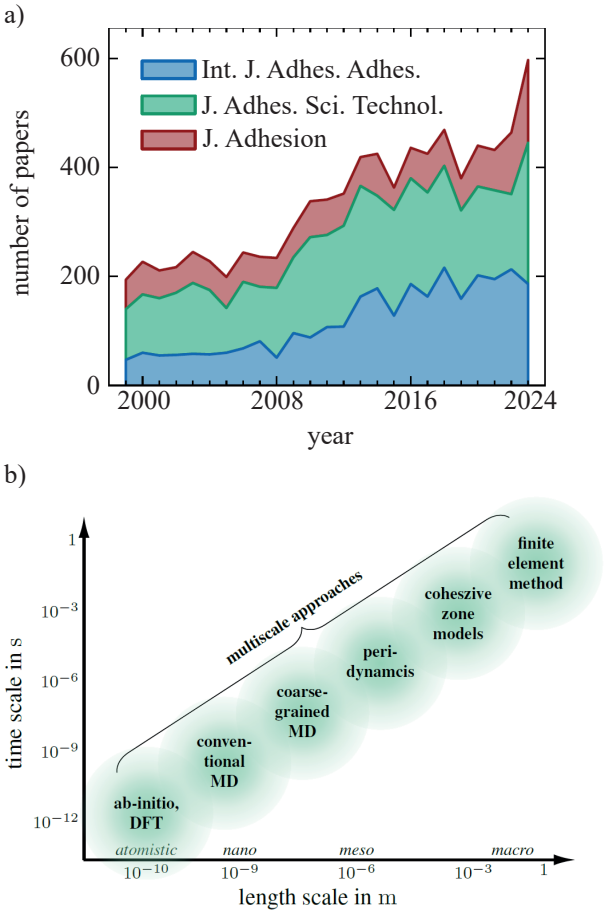

Fig. 1. Number of papers published in "International Journal of Adhesion and Adhesives", "Journal of Adhesion Science and Technology", and "Journal of Adhesion" between 1998 and 2023 (data from SJR – SCImago Journal and Country Rank, https://www.scimagojr.com/) (a), and simulations methods for adhesive joints and the associated length and time scales (b) (inspired by Lin & Wang, 2023)

Researchers have employed particle-based methods like classical and coarse-grained molecular dynamics to unravel the atomistic and nanoscales, while continuum approaches such as peridynamics and finite element-based techniques cover the meso- and macroscale, as illustrated in Figure 1b. The variety of simulation methods reflects the multidisciplinary nature of adhesion science, spanning physical and organic chemistry, material sciences, and engineering (Pocius, 2012).

Scope and outline

This paper aims to provide an overview of the important modeling techniques for adhesive joints and showcase their capabilities and applications. To this end, Section 2 provides a concise overview of the main factors influencing the mechanical behavior of adhesively bonded joints. Section 3 describes molecular dynamics (MD) at atomistic and coarse-grained (CGMD) resolution as the most relevant particle-based method. Section 4 presents continuum-based approaches, focusing on the finite element method (FEM) and the cohesive zone model (CZM). Furthermore, we summarize other FEM-based approaches, such as the virtual crack closure technique (VCCT), phase-field fracture model (PFM), and extended FEM (XFEM). Additionally, we discuss peridynamics (PD) as a promising new method that combines aspects of particle- and continuum-based approaches. Finally, we present multiscale approaches in Section 5. Note that this paper emphasizes particle-based methods, as excellent reviews already cover continuum approaches (e.g. Tserpes et al., 2021 or Wei et al., 2024). Furthermore, we limit this contribution to numerical methods and do not address analytical models, which are comprehensively reviewed by Silva et al. (2009a, 2009b) and Tserpes et al. (2021).

2. Influence factors

In general, the mechanical performance of adhesive joints is primarily expressed by their stiffness, strength, and toughness. Secondary indicators include failure mode, fatigue behavior, and chemical resistance. The mechanical behavior of these joints is influenced by several factors, such as materials used, loading conditions, environmental exposure, and joint geometry, as illustrated in Figure 2. In the following sections, we will briefly explain these factors to provide a basis for understanding the modeling approaches presented later.

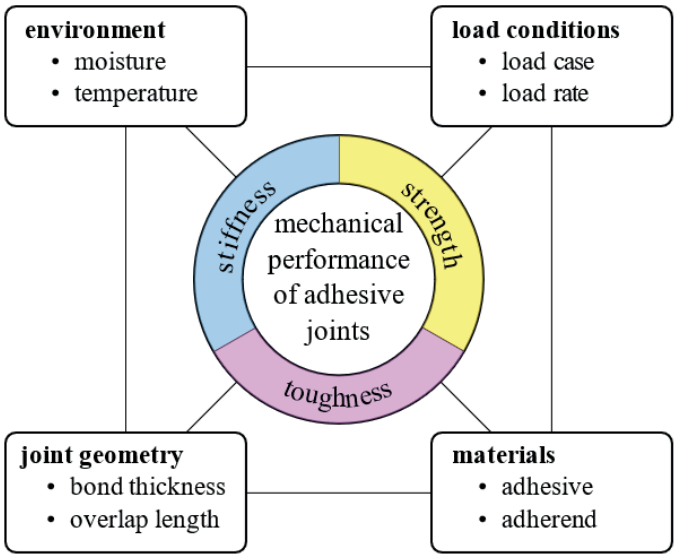

Fig. 2. The mechanical performance of adhesive joints, expressed with the primary indicators stiffness, strength, and toughness is influenced by environment, load conditions, joint geometry, and materials forming a complex network of interdependent influence factors

2.1. Materials

Adhesives

Modern structural adhesives are usually based on acrylics, urethanes, cyanoacrylates, or epoxies, which are highly complex materials (Wei et al., 2024). Epoxies form in the reaction of resin and hardener, with diglycidyl ether of bisphenol A (DGEBA) being one of the most popular resins due to its favorable mechanical properties combined with high chemical, corrosion, and heat resistance. DGEBA can be combined with a plethora of curing agents, such as 4,4′-diaminodiphenylsulfone (DDS) (White et al., 2002), 4,4′-methylenedianiline (MDA) (Shim & Kim, 1997), triethylenetetramine (TETA) (Soliman et al., 2024), diethylenetriamine (DETA) (Possart G. et al., 2009), diethyltoluene diamine (DETDA) (Qi et al., 2006), isophorone diamine (IPD) (Tkachuk et al., 2022), and 4,4-diaminodicyclohexylmethane (PACM) (Shi et al., 2021). Each of these combinations results in a polymer with different properties (Berruet et al., 1987; De Nograro et al., 1995; Garcia et al., 2007) which can be further fine-tuned by choice of curing conditions (Lapique & Redford, 2002), mixing ratios (Haba et al., 2016), and additives (Nemati Giv et al., 2018). This high flexibility leads to many different epoxy-based adhesives with a wide variety of properties and application areas, such as the brittle Araldite AV138 and the ductile Araldite 2015 (Nunes et al., 2015).

Adherends

Besides the adhesive, the adherend material, typically metals (steel, aluminum, copper), carbon-fiber or glass-fiber-reinforced polymers (CFRP, GFRP), or concrete, also significantly affects the behavior of the adhesive bond. Karachalios et al. (2013) compare different steel substrates and found that the failure load of single-lap joints (SLJs) depends significantly on the adherend. While joints with metal adherends typically only exhibit either adhesive or cohesive failure, delamination can occur in joints with FRP adherends (Hasheminia et al., 2019). By joining dissimilar materials, e.g., in CFRP-concrete (Ali-Ahmad et al., 2006) or CFRP-steel bonds (Wang H.-T. & Wu, 2018), the level of complexity increases due to the two different interfaces, resulting in reduced strength compared to similar material joints (Rudawska, 2019).

Surface quality

As the loads are transferred via the substrate surfaces into the adhesive layer, the strength of the bond depends considerably on the adherends' surface quality. Yudhanto et al. (2021) provides a thorough overview of different surface preparation strategies and review their effect on the joint's mechanical properties. In their study on CFRP-steel joints, Shin & Lee (2003) demonstrate the interdependence of influencing factors. They found that while increased surface roughness improves the

strength of double-lap joints (DLJs), it does not lead to any enhancement for SLJs. This is because, in SLJs, out-of-plane peel stresses negate the beneficial interlocking effects associated with higher surface roughness.

2.2. Loading conditions

Load case

Adhesive joints exhibit different behavior when applying out-of-plane (mode I) or in-plane (mode II) deformation, i.e., tensile or shear loading, respectively (Campilho et al., 2013; Floros et al., 2015; Neto et al., 2012). In order to identify the mechanical properties in mode I and mode II, experimental setups are required that allow precise application of the deformation without unwanted mode mixture. Commonly, the double cantilever beam (DCB) is employed for out-of-plane loading, while end-notched flexure (ENF) or double lap joint (DLJ) realizes in-plane deformation. Although being most commonly used due to its simple fabrication, the single-lap joint (SLJ) is not ideal for investigating adhesive joints as the stress state is non-uniform due to out-of-plane stresses caused by the clamping eccentricity (Nunes et al., 2015; Pocius, 2012). To assess the combination of mode I and mode II loading, the mixed-mode bending (MMB) test has been developed, allowing control of the mode mixity α through the length c (Floros et al., 2015), as illustrated in Figure 3.

Load rate

Viscous behavior is a common characteristic of polymers, making the loading rate crucial for adhesive joints, too. Blackman et al. (2012) demonstrate this with their comprehensive study on the effect of load rate in mode I, II, and mixed mode experiments with load velocities from $1 \cdot 10^{-5}$ m·s^{-1} to 15 m·s^{-1}. They observe that the adhesive energy in mode I decreases for increasing load rates while the energy in mode II is unaffected. Furthermore, Karac et al. (2011) distinguish between slow rates <2.5 m·s^{-1} where dynamic effects are negligible and high rates >2.5 m·s^{-1} and identify four regimes of rate-dependent fracture behavior: stable crack growth at slow load rates (<0.1 m·s^{-1}), unstable stick-slip fracture at slow rates (0.1–2.5 m·s^{-1}), continued unstable fracture at high rates (2.5−6.0 m·s^{-1}), and ultimately stable crack growth at high rates (>6.0 m·s^{-1}).

2.3. Joint geometry

The joint geometry, including overlap length, adhesive, and adherend thickness, significantly influences the resulting stress distribution and, consequently, the joint's failure (Shishesaz & Hosseini, 2018). Various contributions confirmed that the adhesive strength decreases for larger bondline thickness (Ji et al., 2010; Silva et al., 2006; Vallée et al., 2006). Possart G. (2014) provides a possible explanation for this thickness dependence by identifying an interphase region adjacent to the adherend with higher stiffness and strength through nanoindentation, cf. Figure 4. Larger overlap length, i.e., a longer adhesive layer, generally increases the joint strength (Vallée et al., 2006). However, this strengthening can be limited by the ductility of the adhesive (Neto et al., 2012) or the adherend (Karachalios et al., 2013).

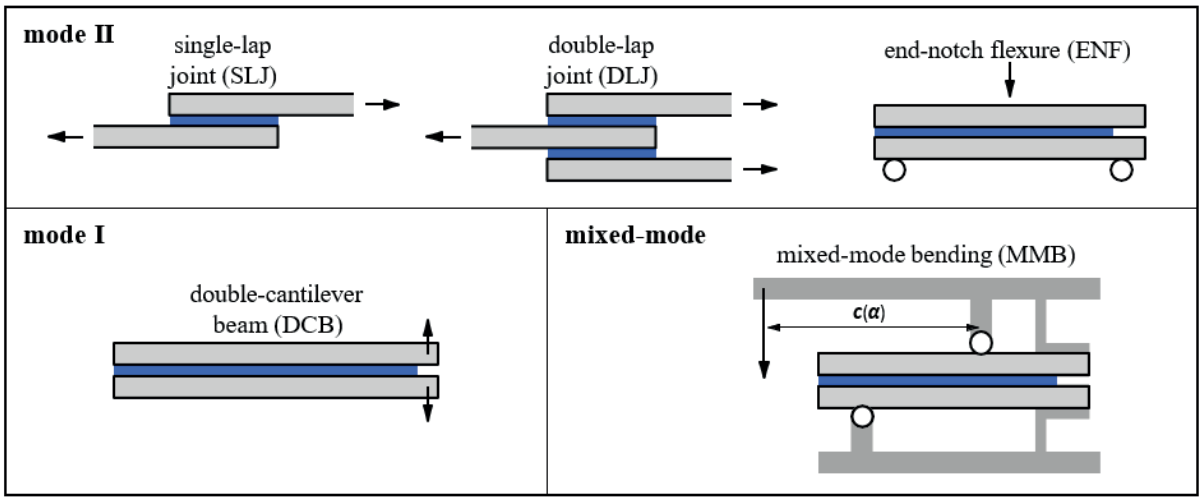

Fig. 3. Common experimental setups for mode I, mode II, and mixed-mode loading

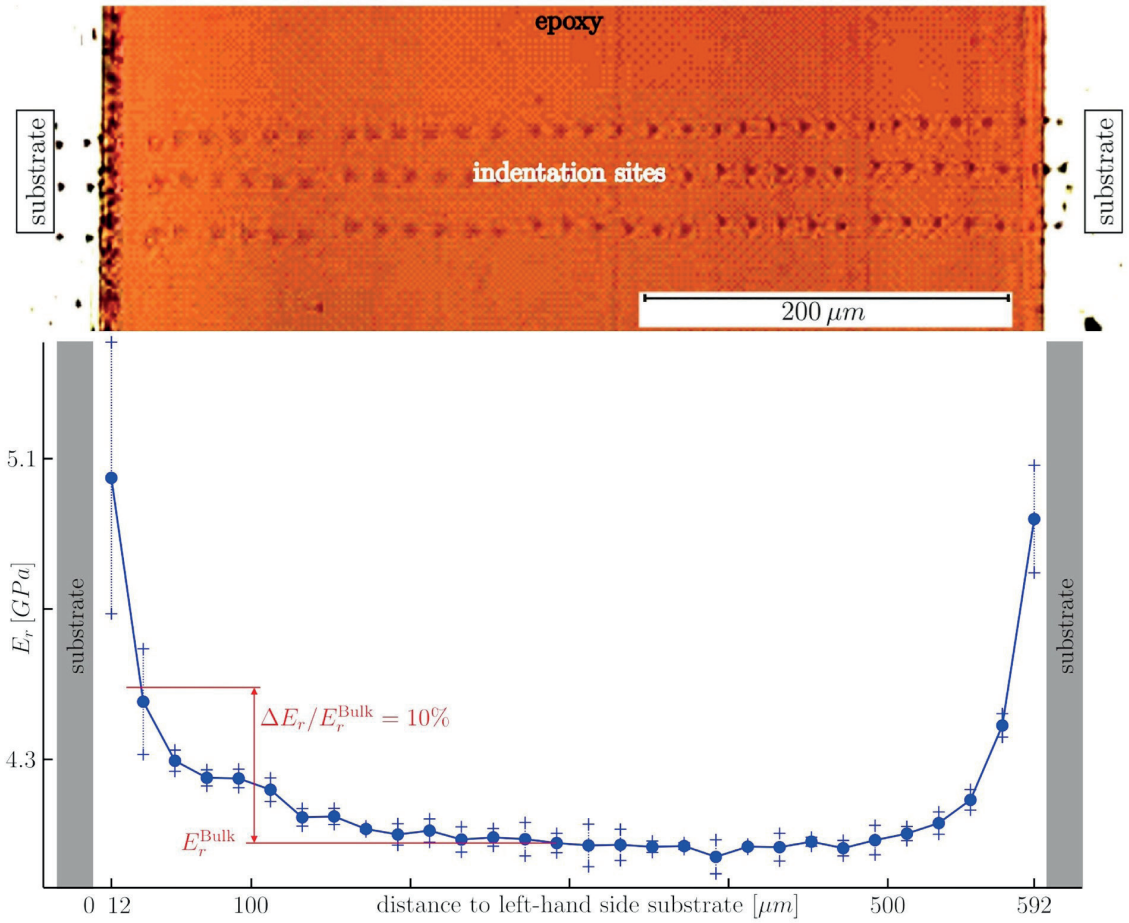

Fig. 4. Experimental interphase identification via nanoindentation: a) light microscopy image of indentation sites; b) resulting local Young's modulus (reprinted from Possart G., 2014)

2.4. Environment

Moisture

In general, moisture negatively affects the mechanical performance of adhesive joints by acting as a plasticizer (Chiang & Fernandez-Garcia, 2002), inducing swelling (Adams et al., 2009), or deteriorating the epoxy network (Xiao et al., 1997). Consequently, the joint's strength decreases with increasing moisture content or exposure time (Armstrong, 1997; Loh et al., 2002).

Temperature

The rate dependency described above inherently implies a temperature-dependent behavior of adhesive joints via the time-temperature superposition principle (Hiemenz & Lodge, 2007). Badulescu et al. (2012) performed mixed mode tensile, compression, and shear experiments from −60°C to 20°C. They observe that lower temperatures significantly increase stiffness and strength but slightly reduce the failure strain. For the high-temperature regime from 20°C to 200°C, Banea et al. (2010) report that strength and toughness reduce with rising temperature.

3. Molecular dynamics

Molecular dynamics (MD) is a popular particle-based method to investigate adhesive joints, or polymeric materials in general, at an atomistic resolution (Vakhrushev, 2018). To this end, Newton's equations of motion are solved for each atom from its interactions with neighboring atoms. These interactions are modeled via potentials, which usually include bond, angle, and dihedral contributions, as visualized in Figure 5. Additionally, nonbonded interactions comprising van der Waals and electrostatic potentials are defined for each atom pair but are typically evaluated only within a certain cutoff radius. We derive the

forces acting on each particle and the associated acceleration from the polymer system's total potential energy. By employing a time integration scheme, such as the Verlet (1967) or Leapfrog algorithm (Frenkel & Smit, 2023), we update the position of all particles for each time step and thus compute the trajectory of our particle system. The time step size is typically in the femtosecond range, so MD simulations are limited to very small time scales. Furthermore, the large number of interactions, caused mainly by the far-reaching nonbonded potentials, leads to high numerical effort and thus constrains the assessable system size. Due to their small dimensions, MD systems have an extreme surface-to-volume ratio. By applying periodic boundary conditions (Allen et al., 2004), we can eliminate free surface effects, which allows for the desired investigation of bulk polymers. Additionally, we impose a thermodynamic state on the MD system using ensembles. Most relevant in this context are the micro-canonical (NVE), canonical (NVT), and isothermal-isobaric (NPT) ensemble, allowing us to control the particle amount (N), volume (V), energy (E), temperature (T), or pressure (P), as visualized in Figure 6. To this end, we rely on thermostats and barostats to regulate temperature and pressure, respectively (Frenkel & Smit, 2023). Some of the most common variants are the Berendsen (Berendsen et al., 1984) and Nosé–Hoover thermostat (Evans & Holian, 1985) and barostat (Martyna et al., 1994). For a more detailed introduction to MD and its associated concepts, we refer to the references (Allen et al., 2004; Frenkel & Smit, 2023; Tadmor & Miller, 2011).

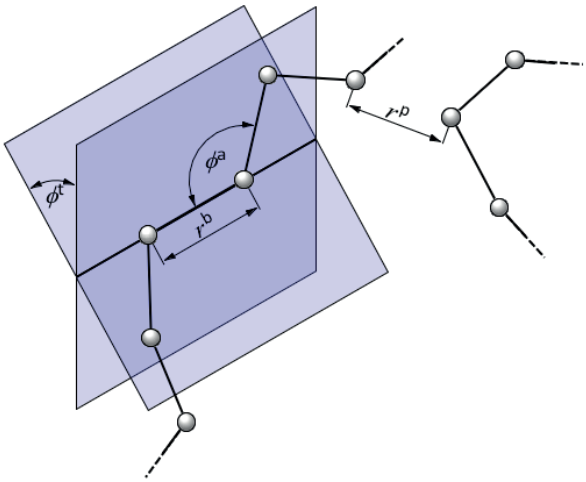

Fig. 5. Parameterization of molecular dynamics interactions between two, three, and four beads via bond length r^b, bending angle ϕ^a, and dihedral angle ϕ^t, respectively, as well as nonbonded interactions with pair distance r^p (reprinted from Ries, 2023)

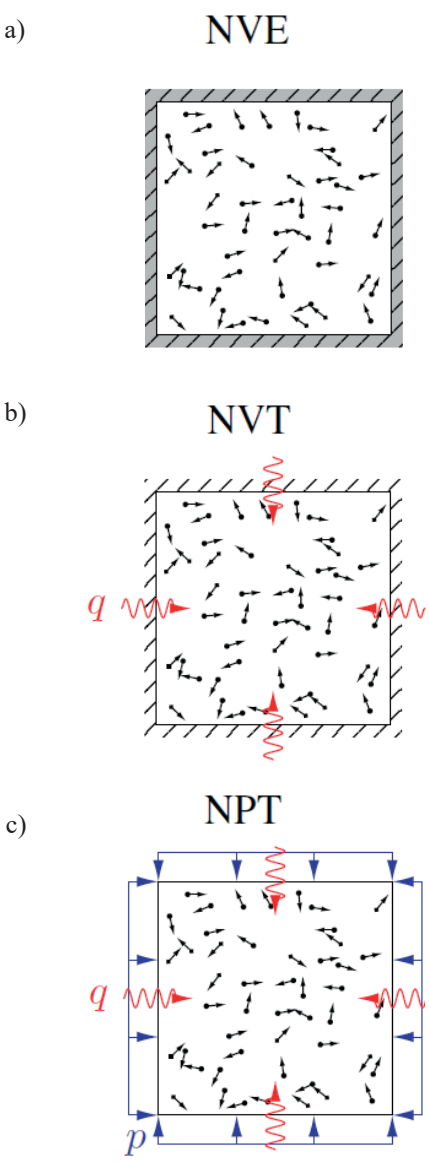

Fig. 6. Thermodynamic ensembles: a) fully isolated system; b) mechanically isolated system in a heatbath; c) closed system in a heatbath represented by micro-canonical (NVE), canonical (NVT), and isothermal-isobaric (NPT) ensemble, respectively, with heat flux q and pressure p (reprinted from Ries, 2023)

In order to characterize the mechanical behavior of a material, an easily accessible measure of the stress state is essential. In MD simulations we rely on the virial stress tensor σ (Thompson et al., 2009).

$$\sigma = -\frac{1}{V}\sum_{i=1}^{n_a}\sum_{\substack{j=1\\ j>i}}^{n_a} f_{ij} \otimes \left[r_i - r_j\right] - \frac{1}{V}\sum_{i=1}^{n_a} m_i v_i \otimes v_j \qquad (1)$$

with total volume V, number of atoms n_a, mass m_i of bead i, force f_{ij} between beads i and j, their positions r_i and r_j, as well as velocities v_i and v_j. The first term contains the virial contributions, which include angle

and dihedral interactions (Tadmor & Miller, 2011), while the second term represents the kinetic contribution. Commonly, we assume that the virial stress coincides with the Cauchy stress commonly employed in continuum-mechanical constitutive laws (Subramaniyan & Sun, 2008; Tadmor & Miller, 2011), which is, however, controversially discussed (Zhou, 2003; Zimmerman et al., 2004). There are three main routes to identify the elastic material parameters with MD: the static, fluctuation, and dynamic approach (Shokuhfar & Arab, 2013). In the static approach (Theodorou & Suter, 1986), we first apply a small deformation to a polymer system in equilibrium, then minimize its potential energy to reach a deformed equilibrium, and derive the elastic coefficients from the potential energy. While this approach is computationally efficient, it fixes bonds and angles and thus neglects entropic effects and thermal fluctuations, limiting its applicability (Theodorou & Suter, 1986). On the contrary, the fluctuation approach employs the Parinello–Rahman (PR) (Parrinello & Rahman, 1982) relation to compute the elastic constants directly from the thermal fluctuations. Since no derivates of the potential energy have to be computed, the fluctuation approach is especially suitable for complex force fields (Gusev et al., 1996). In the context of adhesives, the dynamic approach (Brown & Clarke, 1991) is most popular, as it incorporates thermal and entropic effects and captures not only elastic but also viscous and plastic contributions. Here, a polymer sample is deformed by applying a constant stress (or strain) rate and measuring the strain (or stress) response. The fluctuating response signals are often filtered, for example, using a Savitzky–Golay filter (Savitzky & Golay, 1964), and statistically validated by averaging multiple replicas (Ries et al., 2022). The main drawback is the associated high strain rates (usually in the order of $1 \cdot 10^8$ s^{-1}) that prevent a direct comparison with experiments. Nevertheless, MD seems to capture the molecular mechanisms responsible for the experimental observations and can thus be used to identify relative trends (Sluis et al., 2018). Although there are approaches approximating a quasi-static response from MD (Konrad et al., 2021; Park et al., 2018; Sundararaghavan & Kumar, 2013; Vu-Bac et al., 2015), it remains open whether such simulations can quantitatively predict material behavior as observed in laboratory conditions (Yang & Qu, 2014a). The most popular tool for MD analysis in the scientific community is the open-source software LAMMPS (Plimpton, 1995; Thompson et al., 2022), which facilitates highly customizable simulations through pre-implemented force fields, ensembles, time integration schemes, and output quantities. We categorize MD simulations according to their resolution into atomistic and coarse-grained approaches and start by discussing the former in the following.

3.1. All-atom molecular dynamics (MD)

In all-atom molecular dynamics (MD), every atom is considered a single particle in the simulation, enabling an analysis of the material at atomistic resolution. Force fields describe the interactions between the atoms and model the potential energy landscape using mathematical functions. The force fields must be detailed enough to model the material behavior yet simple enough to allow for a quick numerical evaluation, hence balancing accuracy and efficiency. The force field parameters may be derived from quantum mechanical simulations or by matching experimental data, e.g., obtained from electron diffraction or neutron spectroscopy (González, 2011). Popular force fields with a vast range of applications are CHARMM (Brooks et al., 1983), AMBER (Weiner et al., 1986), Dreiding (Mayo et al., 1990), COMPASS (Sun, 1998), GAFF (Wang J. et al., 2004), and CFF (Maple et al., 1994), which are also commonly employed for modeling polymers. In order to incorporate chemical reactivity, Duin et al. (2001) developed the reactive REAXFF force field, which is of particular importance to model the curing reaction of thermosets. Recently, Livraghi et al. (2023) introduced an efficient GAFF-based block chemistry approach to model the electrostatic interactions during the thermoset's curing, facilitating high cross-linking degrees without needing unphysical interaction ranges. González (2011) provides a more elaborate introduction to MD force fields and their parametrization.

Curing reaction

The mechanical behavior of polymers is strongly influenced by their microstructure, i.e., the arrangement of the polymer chains (Ward & Sweeney, 2012). Thermoplastics feature a microstructure characterized by entanglements (Kröger et al., 2023) and crystalline domains (Bhardwaj et al., 2024; Mészáros et al., 2023), while thermosets consist of a covalently cross-linked network (Jahani et al., 2022; Stewart et al., 2007) created through the chemical reaction of prepolymer and hardener. In order to investigate the mechanical behavior of adhesives with MD, we first have to establish a realistic cross-linked system (Li K. et al., 2016a). In an early static approach, Yarovsky

& Evans (2002) established all bonds within a predefined reaction radius simultaneously, leading to a thermoset with low molecular weight. Wu Ch. & Xu (2006) apply a dynamic bonding approach in which they alternate between energy minimization and MD simulation while establishing favorable bonds individually. Hence, they maintain equilibrium during their network's progressive growth, resulting in highly cross-linked epoxy samples. Varshney et al. (2008) propose a similar dynamic bonding approach but continuously increase the reaction radius. Consequently, high degrees of cross-linking are reached with fewer time steps, saving computational effort and allowing large samples to be generated. Their approach has been successfully employed to study the thermomechanical properties of epoxies (Li K. et al., 2016b; Tam & Lau, 2014).

Neat epoxy

While DGEBA is the standard choice for the epoxy resin in MD studies, its reaction with many different hardeners such as DDS (Liu et al., 2004), MDA (Chang & Kim, 2011), TETA (Tavares et al., 2000), DETA (Shokuhfar & Arab, 2013), DETDA (Clancy et al., 2009), IPD (Wu Ch. & Xu, 2007), or PACM (Shi et al., 2021) has been investigated. Such MD simulations of neat epoxy help to gain a better understanding of their structure-property relation, e.g., by deriving the percolation transition during curing (Livraghi et al., 2021), comparing different hardeners concerning the resulting thermomechanical properties (Jeyranpour et al., 2015), or calibrating continuum mechanical constitutive laws (Park & Cho, 2020). Li Ch. & Strachan (2016) investigate the formation of free volume during curing and its impact on mechanical properties and reveal that a 1% increase in void volume leads to a 10% decrease in stiffness and strength. Similarly, Jang et al. (2022) obtain epoxy samples in good agreement with experiments by applying a pre-deformation that triggers bond-scission and thus induces defects to the polymer network. After an additional equilibration of these damaged samples, they observe that the defects significantly reduce Young's modulus and failure strain. Hence, the explicit modeling of nano-defects offers more realistic predictions of stiffness, strength, and brittle failure as the typically investigated ideal epoxy networks (Jang et al., 2022; Tam & Lau, 2016). Additionally, the curing degree or cross-linking degree, commonly defined as the ratio of the formed to the maximum amount of cross-links, has a major influence on the mechanical properties (Bandyopadhyay et al., 2011). Shokuhfar & Arab (2013) demonstrate that higher cross-linking degrees cause an increase in Young's modulus and a decrease in Poisson's ratio, matching experimental observations.

Due to these promising results on the neat polymer, efforts have been made to address the behavior of adhesive joints. Since these simulations are limited to very small length scales, they examine the immediate vicinity of the adherend- adhesive interface. They investigate various aspects, including the effects of cross-linking and defects, interphase formation, the influence of moisture, and surface chemistry.

Cross-linking

Yang et al. (2013) study the effect of the cross-linking degree on the mechanical behavior of an epoxy-copper interface under tensile loading. They observe that, in contrast to the neat epoxy, the cross-linking does not affect the elastic regime of the bi-material. However, in the post-yielding phase, higher cross-linking leads to higher ultimate stresses since the dense polymer network hinders the initiation and growth of voids. This lack of voids in highly cross-linked systems decreases the ductility, resulting in a lower failure strain compared to samples with a lower conversion degree. Since no covalent bonds between adherend and adhesive were considered in this study, all samples fail adhesively, except those with extremely poor cross-linking which break cohesively.

Interphase

Given its atomistic resolution and accurate modeling of the curing reaction, MD is particularly suited to studying the formation of an interphase. Kanamori et al. (2021) employed all-atom MD simulations to complement their experimental findings on aluminum-epoxy adhesive joints. They observe an interphase region of higher density forming close to the adherend-adhesive interface, contributing to the adhesive strength. Furthermore, they confirm that higher curing temperatures lead to higher curing degrees and, thus, improved mechanical properties. Their MD findings match their laser shock adhesion test (LaSAT) experiments. Li K. et al. (2016a) perform tensile tests on DGEBA-DEDTA bonded to a silica surface with varying cross-linking degrees. They reveal an interphase close to the ad-

herend by evaluating density profiles and radial distribution functions. Moreover, they observe a reduced mobility of the atoms within the interphase, which confirms that the interphase exhibits different material behavior compared to the bulk epoxy. Moreover, higher cross-linking degrees increase the interphase's stiffness and strength, enhancing the adhesion.

Surface chemistry

The atomistic representation of the adherends surface enables the detailed investigation of different surface chemistries with MD. Konrad & Zahn (2023) present accurate, atomistic models for silica-epoxy, cellulose-epoxy, and magnetite-epoxy and compare the polymer network curing near the interfaces for these three adherends. To this end, they perform tensile tests and evaluate the maximum stress and the work of adhesion for quasi-static conditions. They observe a significant weakening of the epoxy at the interface compared to the bulk polymer due to deformation-induced damage and local cavitation of the polymer adjacent to the interface. Steered molecular dynamics (SMD) is an MD-based method where an additional external force is applied to one or more atoms to keep a constant velocity of motion along a selected coordinate (Izrailev et al., 1999). Hence, SMD enables the precise application of a load condition at the molecular scale, making this method particularly suitable for evaluating chain dynamics and mechanical behavior close to interfaces (Min et al., 2017). Deng et al. (2022) employ SMD to compare the interfacial bonding behavior of silica-epoxy with different surface modifications. To this end, they saturate the dangling silica atoms at the adherend surface with hydroxyl (OH) groups reproducing experimental observations. They obtain three more surface configurations by substituting half of the hydroxyl with formyl (COH), carboxyl (COOH), or amine (NH2) groups, respectively. From SMD-driven tensile tests, cf. Figure 7a, they evaluate the interfacial energy E_{inter} over the pulling displacement d as shown in Figure 7b. Evidently, the different functionalizations profoundly impact E_{inter} in the undeformed state ($d = 0$). Furthermore, the interfacial energy flattens when the silica-epoxy joint fails, highlighting the impact of the surface chemistry on the toughness. Finally, only the pure hydroxyl sample features a vanishing E_{inter}, revealing adhesive failure, while the other configurations break cohesively, as indicated by the remaining interfacial energy after debonding.

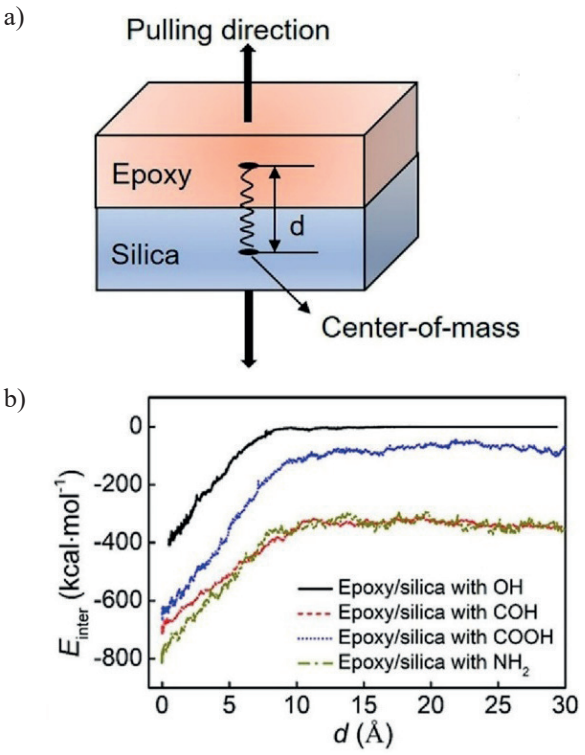

Fig. 7. Examining the surface chemistry with steered molecular dynamics (SMD): a) schematic representation of the SMD setup under tensile load; b) resulting interfacial interactions E_{inter} over pulling displacement d for different surface functionalizations; reprinted from (Deng et al., 2022)

Moisture

In a similar approach, Büyüköztürk et al. (2011) employ SMD to investigate the DGEBA-silica interface in dry and wet conditions. They observe that moisture weakens the joint markedly, as the atomistic adhesive energy drops by 15% in wet conditions for peel and shear tests. Hence, they provide chemistry-based insights into the complex failure behavior of fiber-reinforced polymers bonded to concrete. Tam & Lau (2015) conduct a combined experimental and MD study to identify the effect of moisture on the interfacial properties of photoresist coatings on silica substrates. They demonstrate that the photoresist's Young's modulus is independent of the moisture content, as the water merely fills the voids within the polymer network. However, the free energy profile of the photoresist-silica systems, derived via the metadynamics approach (Laio & Gervasio, 2008), indicates that the moisture severely reduces the adhesion strength. Their experimental investigations confirm these numerical findings, highlighting the potential of MD simulations to complement experiments.

3.2. Coarse-grained molecular dynamics (CGMD)

Coarse-grained MD (CGMD) combines groups of atoms to so-called superatoms (cf. Fig. 8) and calculates their trajectories analogous to conventional MD. The coarsening results in a loss of atomistic accuracy but simultaneously enables the simulation of significantly larger systems, facilitating the mechanical analysis of complex systems, such as adhesive joints. As the established atomistic potentials can no longer be used, the main challenge in coarse-graining is to calibrate the interactions of the superatoms so that the material behavior is reproduced with the necessary accuracy despite the coarsening. CG models are generally material-specific and only valid for the thermodynamic state at which they have been calibrated (Joshi & Deshmukh, 2021). In addition to this transferability problem, CG models exhibit accelerated dynamics due to the softer CG potential, resulting in distortion of dynamic properties, which requires rescaling to be comparable to results from atomistic MD or experiments (Karimi-Varzaneh et al., 2012).

Bottom-up coarse-graining

Bottom-up coarse-graining approaches usually calibrate the coarse-grained potentials to match an atomistic reference solution. The iterative Boltzmann inversion (IBI) (Reith et al., 2003) optimizes the particle-particle interactions to reproduce atomistic radial distribution functions. The multiscale coarse-graining method (MS-CG) (Noid et al., 2008a, 2008b) establishes a mapping from atomistic to CG resolution via the potential of mean force (PMF) while the relative entropy method (Shell, 2016) reproduces the configurational entropy of a fully atomistic reference. The resulting CG potentials usually exhibit mechanical softening, accelerated dynamics, and limited temperature-transferability (Fritz et al., 2011; Karimi-Varzaneh et al., 2012). Xia et al. (2017) provide a remedy by renormalizing the activation free energy via a temperature-dependent rescaling of the nonbonded interactions based on the Adam–Gibbs theory of glass formation. Since this energy renormalization approach amends the CG softening, the resulting CG models are highly suitable for examining the mechanical behavior of thermoplastics (Xia et al., 2019) or epoxies (Giuntoli et al., 2021).

Top-down coarse-graining

In top-down coarse-graining, the potentials are calibrated based on empirical observations and are thus more generic and feature fewer chemical details than bottom-up models (Joshi & Deshmukh, 2021). Many top-down CG approaches are based on the simple Kremer–Grest bead-spring model (Faller et al., 1999; Kremer & Grest, 1990) originally developed for linear chains and thus employed in various CG studies on thermoplastics (Bocharova et al., 2020; Dietz et al., 2022; Moghimikheirabadi et al., 2021; Weber et al., 2024). These models usually employ Lennard–Jones units, i.e., fundamental mass, energy, length, and time, and thus require a back mapping to real units (Everaers et al., 2020; Kröger, 2004) for comparison with experiments.

Neat epoxy

Many studies are developing CG models to analyze the thermo-mechanical properties of neat epoxy. For instance, Yang et al. (2014) calibrate the CG potentials of a simple bead-spring model via particle swarm optimization based on atomistic reference simulations and report good agreement for T_g, density, as well as Young's modulus and Poisson's ratio.

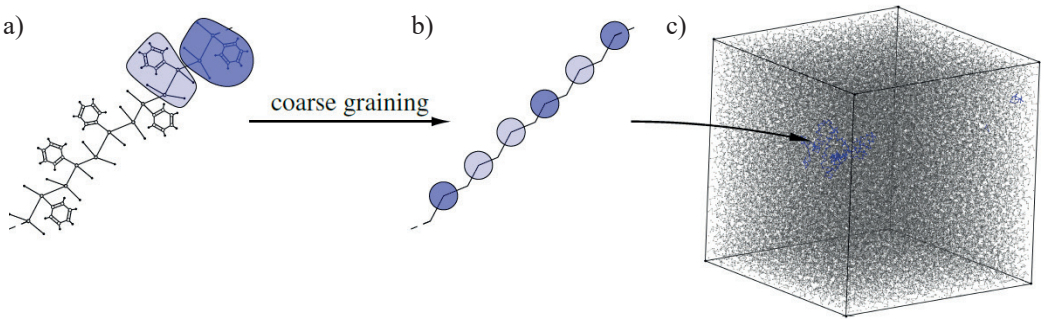

Fig. 8. Coarse-graining with bottom-up strategy exemplary shown for atactic polystyrene: atomistic reference (a) for the parameterization of the coarse-grained model (b), which is subsequently examined in a simulation setup (c) (reprinted from Ries, 2023)

Furthermore, the numerical efficiency of their CG model allows them to analyze the formation of cavities and failure behavior under various loading conditions, which requires length scales not accessible with atomistic MD (Yang & Qu, 2014b). Modeling DGEBA-DAB, Aramoon et al. (2016) optimize bond, angle, and dihedral potentials to represent the energy surface obtained via quantum-mechanical sampling and calibrate the pair interactions to match the experimentally observed density and glass transition temperature. Pal et al. (2023) evaluate how the hardener mix of PACM and Jeffamine influences the curing of DGEBA and the resulting mechanical behavior at CG resolution (Giuntoli et al., 2021). They perform tensile simulations until rupture and observe that PACM mainly affects the stiffness, while short and long Jeffamine chains increase the strength and toughness, respectively. Another approach employs dissipative particle dynamics (DPD) (Español & Warren, 1995; Groot & Warren, 1997), which adds dissipative and random forces to the conservative Newtonian interactions between particles. Kacar et al. (2013) introduce a CG-DPD parametrization scheme and apply it to derive the CG potentials for DGEBA-DETA. The resulting efficient CG-DPD model allows for long-time equilibration of large systems, which are backmapped to the atomistic scale, resulting in sample sizes not feasible by conventional MD. They demonstrate that the elastic and thermal properties obtained via this backmapping approach are in good agreement with the experimental values. Similarly, Gavrilov et al. (2014) developed a DPD coarse-graining scheme based on neural-gas networks and Hebbian learning, allowing a detailed analysis of the epoxy network after a backmapping to atomistic resolution is performed. Yagyu et al. (2012) elucidate the cross-linking dependence of a chemically amplified, epoxy-based photoresist by means of a bead-spring model. They compute Young's modulus from uniaxial tension tests and observe a linear relation between stiffness and cross-linking degree matching their nanoindentation experiments.

Cross-linking

In contrast to the atomistic MD studies cited earlier, which typically simulate only one substrate, CGMD is more efficient and can predict the adhesive properties between two adherend surfaces. The balance between molecular detail and computational cost makes CGMD particularly suitable for investigating the structure-property relation of adhesive layers and its impact on the load-bearing capacity and failure behavior of joints. For example, Stevens (2001) studies the impact of the covalent bond density between adherend and adhesive on the failure of the joint utilizing a simple bead-spring model. He concludes that failure strain and stress are proportional to the interfacial bond density for tensile and shear loading. Moreover, he reports that the van der Waals interactions only influence the tensile behavior for scarcely bonded interfaces and do not contribute under shear loading. Similarly, Solar et al. (2014) employ a simple Kremer–Grest model to evaluate how the number of cross-links affects the mechanical performance of an adhesive joint. While stiffness and strength increase monotonically with the number of cross-links, the failure strain reaches its maximum for intermediate curing degrees. This peak in ductility coincides with the transition from cohesive to adhesive failure, which is observed for low and high cross-linking degrees, respectively. Raos & Zappone (2024) employ a spring-bead model to investigate the effect of cross-linking and surface grafting on the work of adhesion and failure mode of a generic adhesive joint. They conclude that cross-links are more important in improving adhesion than the covalent bonds between adherend and adhesive. Moreover, they observe that surface heterogeneities, i.e., inhomogeneous grafting bond distributions, lead to a considerable reduction in strength and, thus, smaller work of adhesion. For the same model, Baggioli et al. (2020) attribute this weakening to the formation of cavities, which are most likely to nucleate at the adherend surface for highly heterogeneous surface morphologies. They perform uniaxial tensile tests of the generic epoxy bonded to two rigid surfaces until failure, as depicted by the snapshots in Figure 9a. The spatial arrangement of weakly and strongly interacting sites at the adherend surfaces has a significant impact on the mechanical behavior of the adhesive joint, cf. Figure 9b. Homogeneous distributions, i.e., either fully random ($\alpha = 0$) or checkerboard patterns ($\alpha = -1.0$), yield high adhesive strength, while the mechanical performance deteriorates for increasing segregation of the reaction sites ($\alpha > 0$). Jin K. et al. (2018) investigate the failure mode of pressure-sensitive adhesives and report that a high curing degree results in a strong adhesive, leading to early adhesive failure. On the contrary, sparse cross-links cause early cohesive failure of the adhesive. Thus, the failure behavior can be controlled via the curing reaction, with an optimum toughness obtained at medium cross-linking degrees.

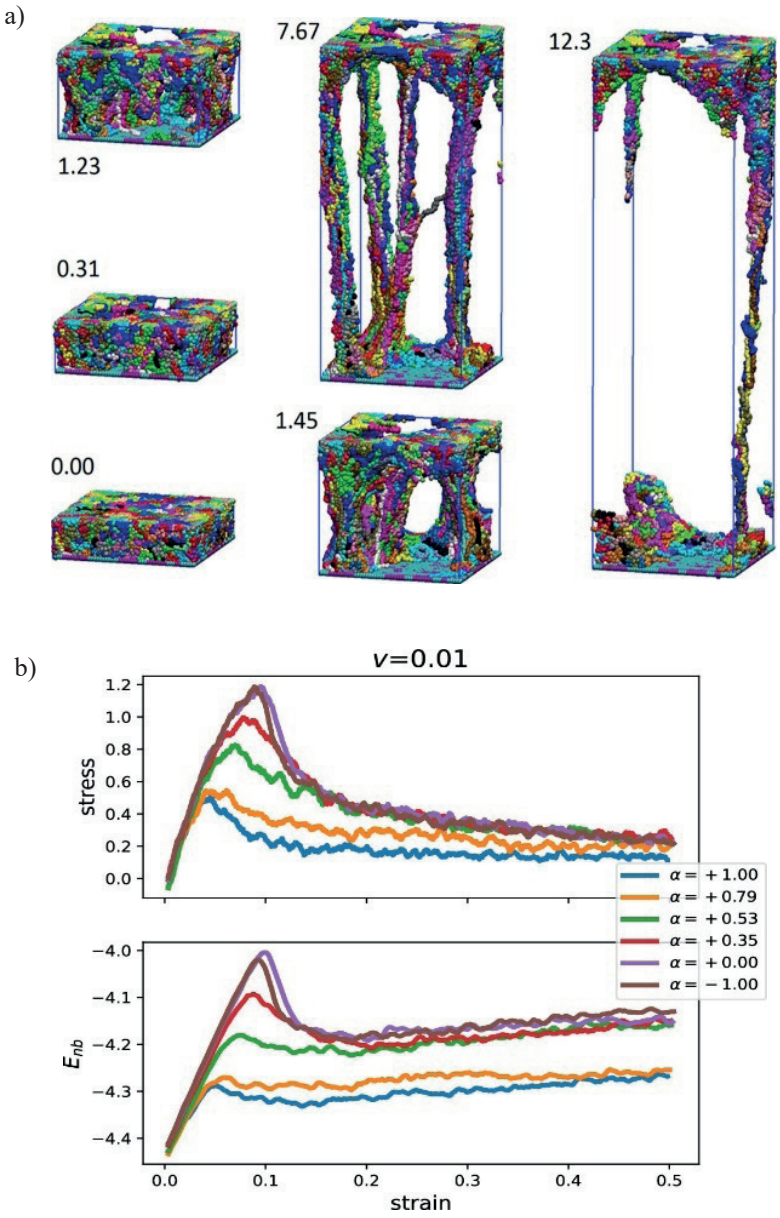

Fig. 9. Coarse-grained molecular dynamics study: a) failure of a polymer film between two adherends (not visualized) at different strain levels; b) corresponding stress and nonbonded energy between polymer and substrate for different surface morphologies, checkerboard (α = −1), random (α = 0), and heterogeneous (α > 0); reprinted from (Baggioli et al., 2020)

Interphase

Langeloth et al. (2015) calibrate CG potentials for DGEBA-DETA via iterative Boltzmann inversion and investigate the curing in the presence of a rigid substrate. In the vicinity of a substrate, they detect substantial variations of the local epoxy-hardener ratio and associated deviations in the local curing degree compared to the bulk polymer. This structural interphase depends on the epoxy-substrate interactions and affects the local glass transition temperature at a distance of 3–4 nm from the substrate, implying a mechanical weakening. Li M. et al. (2013) develop a CG-DPD approach to investigate the interplay of cross-linking and diffusion during the curing of carbon fiber-reinforced DGEBA-DDS. They observe a markedly reduced cross-linking density near the fiber surface, indicating an interphase region. From the distribution of the cross-links, they derive an interphase thickness of 70 nm, which is in good agreement with their experimental results from energy-dispersive X-ray microanalysis (EDX).

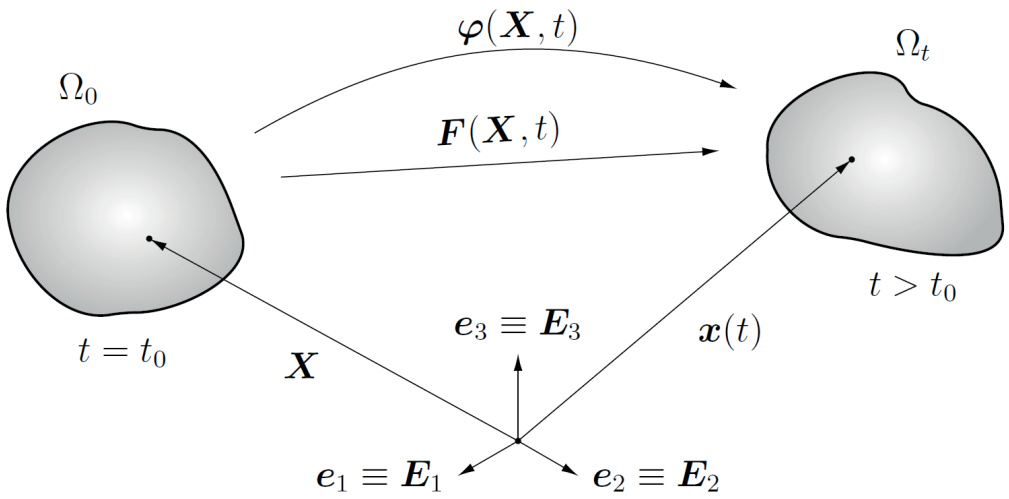

Fig. 10. Standard continuum mechanical setup: initial Ω_0 and current configurations Ω_t at time t_0 and $t > t_0$, respectively, with corresponding position vectors $\boldsymbol{X}$ and $\boldsymbol{x}(t)$, deformation map $\varphi(\boldsymbol{X}, t)$, and deformation gradient $\boldsymbol{F}(\boldsymbol{X}, t)$ (reprinted from Ries, 2023)

4. Continuum-based methods

Contrary to these particle-based approaches, continuum methods do not consider the actual molecular microstructure but model the material as spatially continuous matter. This approximation significantly reduces the numerical costs and thus enables the investigation of engineering problems at the meso and macro scales. The foundation of these techniques is provided by nonlinear continuum mechanics (Holzapfel, 2000; Tadmor et al., 2012), which considers a body in undeformed Ω_0 and deformed configuration Ω_t with position vectors $\boldsymbol{X}$ and $\boldsymbol{x}$, respectively, as visualized in Figure 10. The mapping between these configurations is established via the deformation gradient $\boldsymbol{F} = \partial x / \partial X$, from which we derive common strain measures, e.g., the right Cauchy–Green tensor $\boldsymbol{C} = \boldsymbol{F} \cdot \boldsymbol{F}^t$ or the Green–Lagrange tensor $\boldsymbol{E} = [\boldsymbol{F} \cdot \boldsymbol{F}^t - \boldsymbol{I}]/2$, with identity $\boldsymbol{I}$. By linearizing $\boldsymbol{E}$, we recover the commonly used engineering strain tensor $\varepsilon = [[\boldsymbol{F} - \boldsymbol{I}] + [\boldsymbol{F} - \boldsymbol{I}]^t]/2$. Additionally, we consider external loads and employ Cauchy's theorem to derive the Piola $\boldsymbol{P}$ and Cauchy $\boldsymbol{\sigma}$ stress tensors, which describe the stress state in the undeformed and deformed configuration, respectively. The relation between the stresses and strains is given by constitutive laws, which provide mathematical formulations to capture one of the four paradigmatic material models: elasticity, plasticity, viscoelasticity, or viscoplasticity (Steinmann & Runesson, 2021). A plethora of different constitutive laws has been developed to model the complex behavior of polymers, ranging from nonlinear elastic (Treloar, 1975) to highly complex viscoelastic-viscoplastic models (Bergstrom & Bischoff, 2010; Zhao et al., 2021), as showcased in the comprehensive overview by (Ward & Sweeney, 2012). Continuum-based methods typically solve the boundary value problem derived from the balance of linear momentum in a numerically discretized fashion.

4.1. Finite element method (FEM)

One of the most popular continuum-based techniques in engineering is the finite element method (FEM), which discretizes the simulation domain into finite elements, solves the governing equations element-wise, and assembles the element contributions into a global solution (Zienkiewicz & Taylor, 2005). There are both commercial FEM software, e.g., Simulia Abaqus and Ansys, and open-source libraries such as deal.ii (Africa et al., 2024) or MoFEM (Kaczmarczyk et al., 2020). Due to the high degree of flexibility regarding geometry, boundary conditions, material models, and the comparatively high computational efficiency, FEM is widely used for the macroscale analysis of adhesives. Firstly, we present two pure FEM studies that model the behavior of the adhesive layers solely by modifying the constitutive relations. Possart G. (2014) performs comprehensive FEM simulations of adhesive joints to extract the local interphase material properties from experimental results. To this end, they explicitly model the interphase via property gradients, as shown in

Figure 11, which are motivated by SEM-based shear tests. They conclude that the plastic material parameters are mainly affected within the interphase and qualitatively assess suitable property profiles. Furthermore, they conduct nanoindentation tests and deduce that, in addition to the inherent effects of the substrates, there must be a grading of the properties within the interphase, visualized in Figure 4. They conclude that these experiments offer sufficient resolution to detect the interphase, but that complementary simulations are required to differentiate between interphase and substrate effects, in order to accurately identify the interphase's properties. In another experimentally-motivated study, Schmelzle et al. (2023) extend the toughened adhesive polymer (TAPO) constitutive model to capture adhesive joints' highly temperature-dependent material behavior. To this end, they consider two crash-optimized structural polymers and first identify the material parameters at single temperatures from experimental data. Subsequently, they use the obtained parameters to calibrate temperature-dependent functions for each material parameter individually. These two steps are repeated iteratively to capture interactions between material parameters, resulting in a robust identification procedure. The resulting extended material model accurately reproduces the experimentally observed behavior over a wide range of temperatures.

FEM-based methods

There are several approaches to extending the FEM so that the failure of adhesive joints under different loading conditions can be simulated. The virtual crack closure technique (VCCT) (Krueger, 2015; Rybicki & Kanninen, 1977) is based on linear elastic fracture mechanics; thus, the propagation of a required initial crack is driven by the critical energy release rate, usually obtained in experiments. Jokinen et al. (2015) obtain a good match between VCCT and experiments for the failure of aluminum-epoxy DCB, thus confirming VCCT's applicability to adhesive joints. Senthil et al. (2018) successfully employ VCCT to model the initiation and growth of debonds in adhesive joints under axial compression. De Carvalho et al. (2019) combine VCCT with a nodal release strategy to reduce stress concentrations and to overcome the mesh-dependent crack growth. They validate their method by investigating the fatigue-induced delamination growths in DCB, ENF, and MMB simulations.

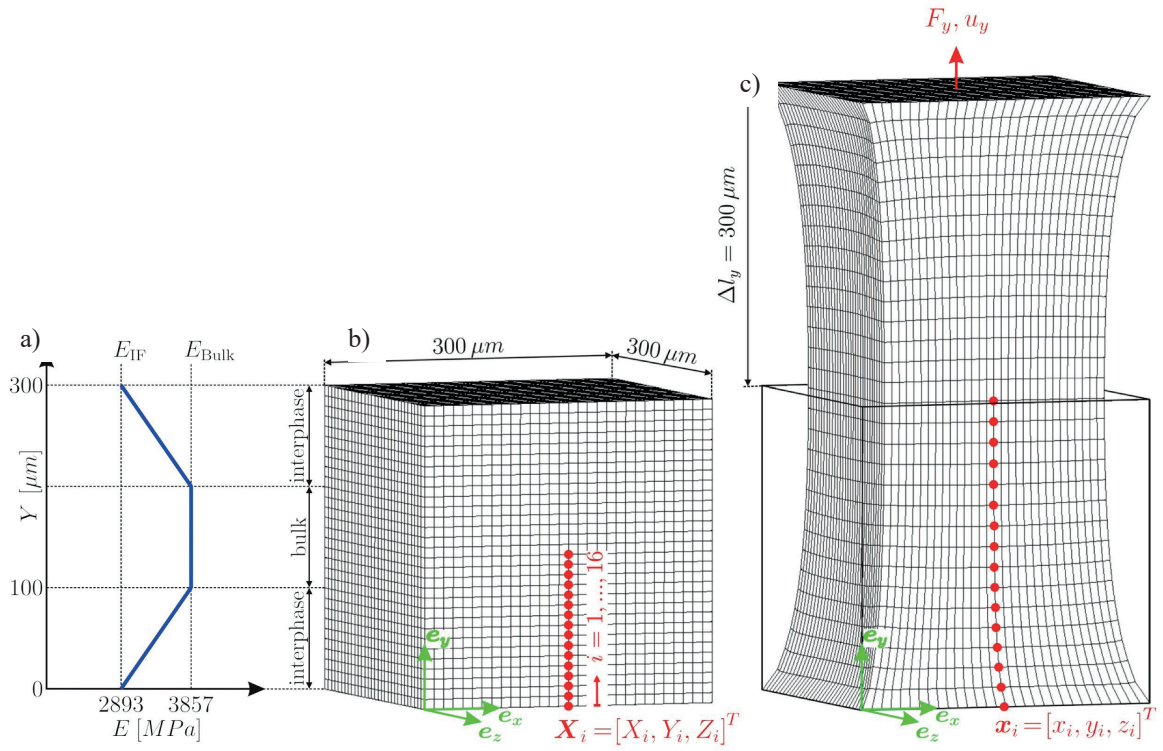

Fig. 11. Finite element analysis of an adhesive joint with property gradients within the interphase (a), undeformed (b) and deformed configuration (c) (reprinted from Possart G., 2014)

Contrary to VCCT, the extended FEM (XFEM) (Belytschko & Black, 1999; Moës et al., 1999) does not require a precrack and allows for discontinuities within an element by additional degrees of freedom. Therefore, the XFEM mesh does not affect the crack propagation, making this method appropriate for fracture simulations of adhesive joints. Campilho et al. (2011a) confirm the feasibility of XFEM for predicting the strength of DCB specimens but conclude that XFEM is not suited for modeling damage propagation as cracks will follow the maximum principal stress direction and thus grow towards the adherends (Campilho et al., 2011b). In a recent contribution, Santos et al. (2023) employ XFEM to examine the failure mode and strength of glass bead-reinforced adhesives. The addition of the glass fillers weakens the SLJ but allows the adjustment of the failure mode from adhesive to cohesive as stress concentrations surrounding the fillers attract the crack tip, as shown in Figure 12. Their XFEM model accurately reproduces experimental results, including the substrate's plastic yielding.

The phase-field fracture model (PFM) (Bourdin et al., 2000; Miehe et al., 2010) replaces the sharp crack of Griffith's theory (Griffith, 1921) by a diffused damage zone characterized by an auxiliary phase field variable and an additional internal length scale parameter. The governing equations are commonly numerically solved with the FEM, and PFMs are increasingly popular for investigating fracture mechanics problems (Li P. et al., 2023). Shi & Zhang (2024) reformulate the PFM length scale parameter in terms of the material strength and simulate the failure of DCBs with GFRP and steel substrates. The resulting load-displacement curves and the crack paths are in excellent agreement with experiments showcasing the ability of PFM to model adhesive joints.

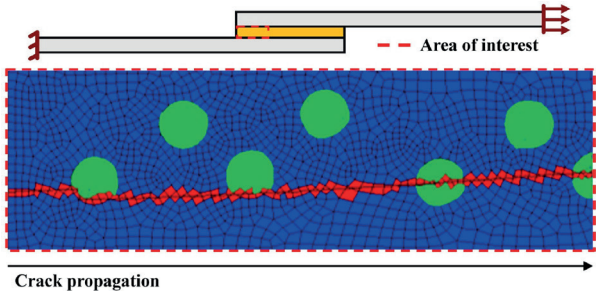

Fig. 12. Failure of a single-lap joint (SLJ) with adhesive containing 10 vol.% glass beads, damage path obtained by extended finite element method (XFEM) highlighted in red (reprinted from Santos et al., 2023)

4.2. Cohesive zone model (CZM)

The most commonly used continuum method for investigating adhesive bonds is the cohesive zone model (CZM) introduced by Barenblatt (1962) based on linear elastic fracture mechanics (Griffith, 1921). Originally developed for brittle fracture, Dugdale (1960) expanded CZM to ductile materials by considering a process zone at the crack tip. Finally, Hillerborg et al. (1976) introduced the cohesive tractions through a traction-separation law (TSL) and solved the CZM problem using FEM. Typically, the adherends are modeled with conventional constitutive laws, while the adhesive is governed by a TSL, allowing to capture damage initiation and propagation, as shown in Figure 13a. The TSL incorporates all fracture-related mechanisms in the process zone ahead of the crack tip, such as crazing, plastic deformation, and crack coalescence in a homogenized fashion (Lau et al., 2012). Hence, the shape of the TSL has a crucial impact on the damage propagation (Campilho et al., 2013), and thus, various functions have been proposed to capture the subtleties of different materials. The most prominent are triangular (bi-linear) (Alfano & Crisfield, 2001), linear-parabolic (Allix & Corigliano, 1996), polynomial (Chen, 2002), exponential (Chandra et al., 2002), and trapezoidal (Campilho et al., 2008) functions. The main advantages of CZM are that damage initiation and growth are modeled without assumptions regarding their location and direction, making CZM easily applicable to complex geometries and load cases (Floros et al., 2015). Furthermore, there are many different failure criteria available (Ascione & Mancusi, 2010), and the effects of load rate (Ascione & Mancusi, 2010) and moisture (Katnam et al., 2010) can be incorporated. Additionally, there are closed formulae to derive the failure load and optimal bonding length (Mancusi & Ascione, 2013). The main drawbacks are the CZM's mesh dependency, the non-unique choice of TSL shape (Jaillon et al., 2019), and the required parameter calibration (Floros et al., 2015). For a triangular TSL as shown in Figure 13a, we need to identify the initial stiffness, the adhesives strength, i.e., the peak traction, and the fracture energy corresponding to the area enclosed by the traction-separation curve. While the stiffness and strength are typically obtained from simple experiments on adhesive dogbone samples, the fracture energy is measured in more complex test setups, such as DBC, ENF, or MMB (Wei et al., 2024). Commonly, we determine these TSL parameters separately for mode I and mode II conditions and employ coupling criteria for damage initiation (Campilho et al., 2013; Floros et al., 2015; Khoramishad et al., 2010) and propagation (Hutchinson & Suo, 1991) to interpolate the mixed mode response, as visualized in Figure 13b.

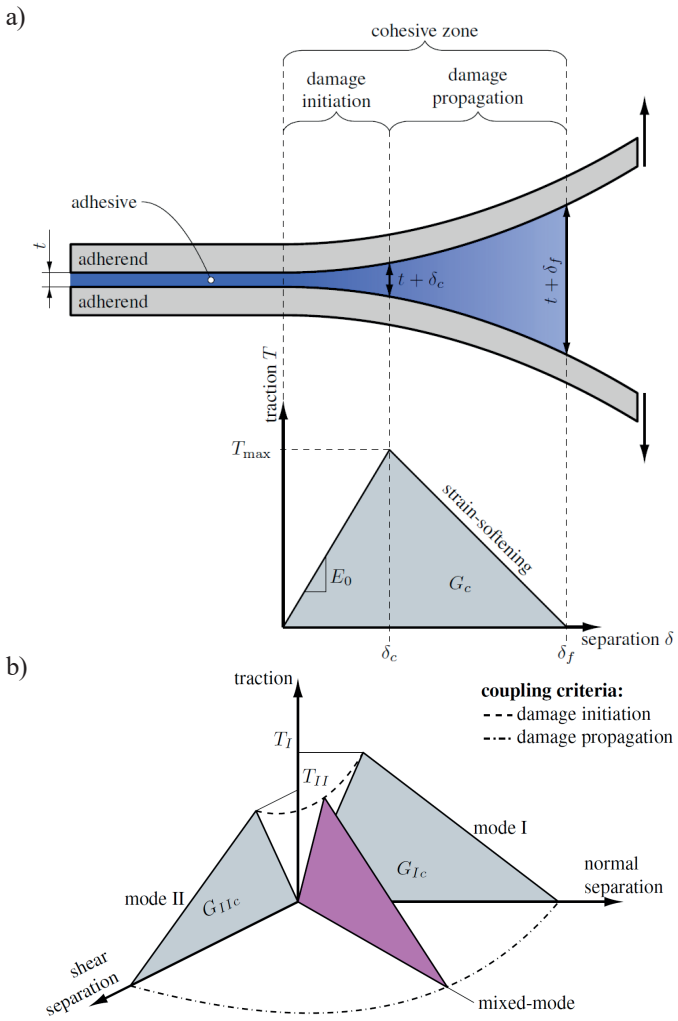

Fig. 13. Cohesive zone modeling (CZM): a) double-cantilever beam with adhesive of thickness t bonding two adherends, in the cohesive zone the traction-separation law (TSL) governs the damage initiation until maximum traction T_{max} is reached at separation δ_c, and subsequent damage propagation with strain softening until failure separation δ_f with $T = 0$ and adhesive energy G_c; E_0 is a traction divided by separation b) mixed-mode TSL derived from mode I and mode II via damage initiation and propagation coupling criteria (both inspired by Khoramishad et al. 2010)

The following examples should demonstrate the CZM's wide applicability in modeling the behavior of adhesive joints. With currently more than 1400 scopus-listed contributions, this excerpt is by no means exhaustive, and the reader is referred to recent CZM-specific review papers, e.g., by Tserpes et al. (2021) or Ramalho et al. (2022). Nunes et al. (2015) compare the tensile performance of three commercial adhesives in SLJ and DLJ tests. They derive the parameters of a triangular TSL from these experiments and employ CZM to evaluate the through-thickness normal and shear stresses. Similarly, Li Ch. et al. (2019) conduct a combined experimental and numerical study on CFRP-steel joints and compare the performance of different adhesives. They show that the strength, bond-slip, and failure mode of SLJ depend on the adhesive's properties and obtain good CZM predictions as long as no delamination occurs in the FRP substrate. Employing CZM to model the failure of tapered DCBs at different load rates, Karac et al. (2011) conclude that a rate-independent TSL can be applied for stable fracture behavior, while stick-slip fracture is only captured with a rate-dependent adhesive energy model which considers the heat affected zone.

Joint geometry

Fernandes et al. (2015) perform SLJ tests to evaluate the impact of the overlap length on the joint strength for three adhesives with different ductility. Larger overlap length leads to higher strength, which is more pronounced for ductile adhesives and can be accurately predicted with CZM. Neto et al. (2012) analyze the failure of SLJ with fiber-composite adherends and observe that ductile adhesives exhibit increased strength for larger overlap lengths. In contrast, brittle adhesives reach a strength plateau due

to delamination in the adherends. They obtain accurate strength predictions for the brittle adhesives using triangular CZMs but report larger deviations for the ductile adhesive and suggest using a trapezoidal TSL instead. Similar results are obtained by Ribeiro et al. (2016), which capture the impact of overlap length on the strength and failure of CFRP-aluminum bonded with brittle and ductile adhesives. CZM is successfully employed to capture the impact of the adhesive thickness on the cohesive parameters and the overall strength for SLJ (Xu & Wei, 2013) and scarf joints (Liao et al., 2013). Moya-Sanz et al. (2017) employ CZM to simulate SLJs with different geometrical configurations and observe the highest strength when chamfering both adherend and adhesive by 15°.

Environment

Banea et al. (2011) study the fracture toughness of DCB at elevated temperatures up to 100°C and calibrate a triangular TSL with temperature-dependent parameters. The adhesive strength decreases with increasing temperature, while the fracture toughness only declines drastically above T_g, which is accurately captured by their CZM simulations. Sugiman et al. (2013) successfully propose a moisture-dependent triangular TSL to predict the residual strength of adhesive joints after aging in deionized water. Similarly, Han et al. (2014) employ degraded CZM parameters to capture the ageing effect on adhesive joints in combined thermal-hygro-mechanical service conditions.

Recent studies

In very recent contributions, Schmandt & Marzi (2025) extend CZM to capture thick adhesives and stick-slip instabilities, Wang Ch. et al. (2025) propose a modified exponential TSL incorporating the real contact area to simulate rough surfaces, and Saikia & Muthu (2024) propose a modified compact-tension test procedure to identify all CZM parameters with one common, simplified experimental setup. Moreover, Abdalla et al. (2025) employ CZM to elucidate the effect of graphene nanoplatelet reinforced adhesives and Wu Y. et al. (2025) successfully apply CZM to simulate bonded bone with hydrogel adhesives for future medical fracture treatment.

Generalized interfaces

While CZM only accounts for displacement jumps at the interface, generalized interface models (GIM) allow for additional traction jumps (Esmaeili et al., 2017). Therefore, GIMs are suitable for complex load histories, e.g., stretching parallel to the interface and subsequent mixed mode loading, as demonstrated by Spannraft et al. (2022) for small and large deformations (Spannraft et al., 2023). The degradation of the interface during the in-plane load does not result in an interface separation, which conventional CZM would not capture. Saeb et al. (2021) augment GIM with weighted average operators which effectively model material property gradients as observed in the interphase of adhesive joints (Possart W. et al., 2006) or polymer nanocomposites (Ries et al., 2021). Hence, this extension enables substituting spatially finely resolved interphase regions with efficient interfaces. Firooz & Javili (2019) provide a review on GIMs for modeling composite materials.

4.3. Peridynamics (PD)

Peridynamics (PD) is a novel continuum approach to resolve the problems arising from singularities in fracture mechanics (Silling, 2000). Contrary to classical continuum mechanics, as introduced in Figure 10, PD is a nonlocal theory, which means that each material point interacts with its finite size neighborhood, as shown in Figure 14. Hence, PD combines the modeling strategies of particle and continuum approaches and can be interpreted as upscaled MD (Laurien et al., 2023), with the size of the neighborhood defining the degree of nonlocality. Since the original bond-based PD (Silling, 2000) is limited to a fixed Poisson's ratio, more advanced versions such as the state-based (Silling et al., 2007) and continuum-kinematics-inspired PD (CPD) (Javili et al., 2019) have been developed. These extensions were successfully applied to biomedical applications (Schaller et al., 2022), failure of porous materials (Ritter et al., 2023), and multiphysics modeling (Xia et al., 2021). Recently, Ma et al. (2023) incorporate a TSL into state-based PD to describe the interfacial failure of composite materials via a zero-thickness interface. Contrary, Laurien et al. (2024) consider a finite-size interface, where the constituents overlap, and introduce a thermodynamically consistent extension to CPD, which can integrate any TSL from the literature. Dorduncu (2020) successfully employ PD to model adhesively bonded CFRP and aluminum beams with functionally graded adhesive layers and Behera et al. (2021) study the damage initiation and progression in SLJs and DLJs with viscoelastic adhesives. Although not yet as refined as CZM, these examples illustrate that PD offers a promising novel approach to investigating the complex behavior of adhesive joints.

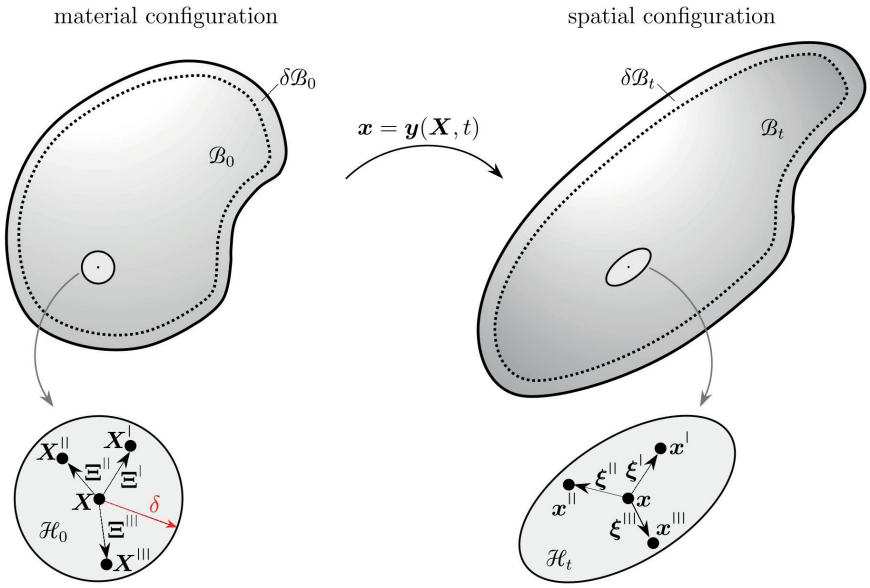

Fig. 14. Continuum-kinematic-inspired peridynamics with material B_0 and spatial configuration B_t, where each point $\boldsymbol{X}$ interacts with its material H_0 or spatial event horizon H_t of radius δ (reprinted from Laurien et al., 2024)

5. Multiscale approaches

Multiscale approaches typically consider a fine and a coarse scale. While the fine scale resolves the microstructure in detail, providing deep insights into the material behavior, the coarse scale is computationally less expensive and only captures the overall response. The challenge of multiscale techniques is the efficient transfer of boundary conditions applied on the coarse scale to the fine scale and vice versa, conveying the insights gained at the fine scale back to the coarse scale. Tadmor & Miller (2011) categorize multiscale methods into sequential and concurrent approaches, with the latter further subdivided into hierarchical and domain-decomposition techniques, as shown in Figure 15.

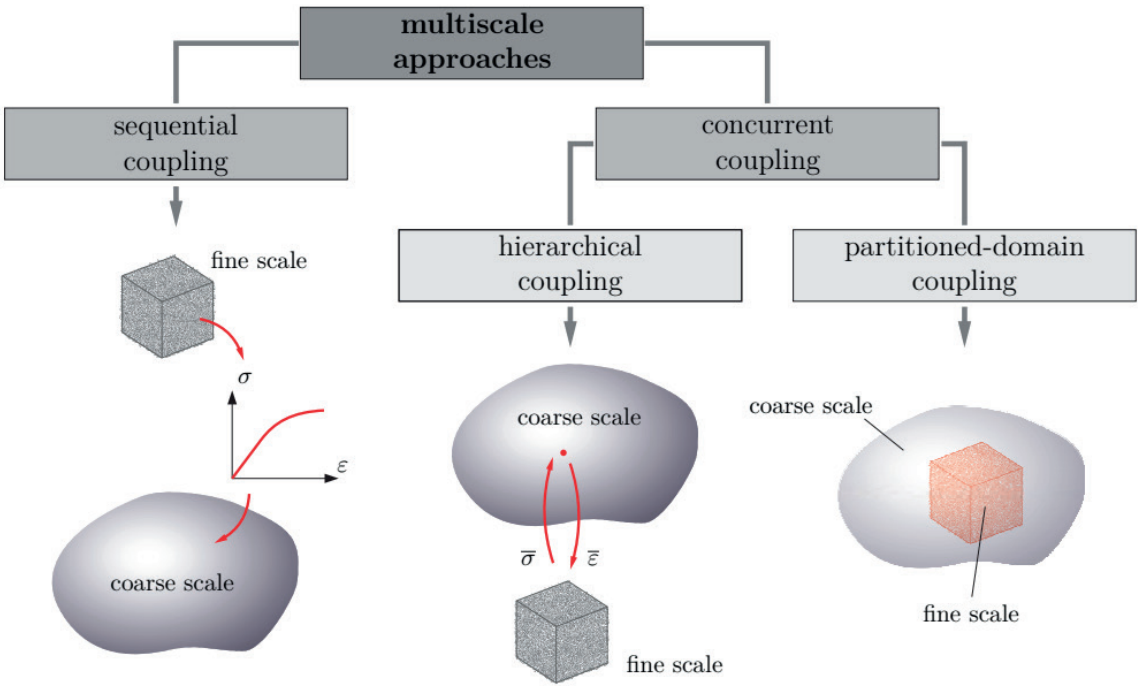

Fig. 15. Classification of multiscale strategies according to Tadmor & Miller (2011) (reprinted from Pfaller, 2022)

In hierarchical methods, both scales are resolved simultaneously, e.g., with the prominent FE^2 approach (Feyel, 1999; Smit et al., 1998) that solves a fine scale boundary value problem for each quadrature point at the coarse scale. Hence, the FE^2 method is beneficial for macroscopically homogeneous materials with complex, heterogeneous microstructures, such as composites (Meng et al., 2024; Zernsdorf et al., 2024). In recent studies, the method's main drawback of high computational cost is remedied by employing machine-learning techniques (Chaouch & Yvonnet, 2024; Lu et al., 2018). On the contrary, domain-decomposition approaches resolve only regions of interest at the fine scale and employ the computationally efficient coarse description for the remainder of the domain. Notable examples, such as the Quasicontinuum (Tadmor et al., 1996) and Capriccio method (Weber et al., 2023) are thus well suited to study the fracture behavior of crystalline (Ghareeb & Elbanna, 2020) and amorphous (Weber et al., 2025) materials, respectively. However, in the context of adhesive joints, there is no clear region of interest for a domain decomposition, and the macroscopic adhesive-adherend interface is not suitable for a hierarchical treatment. Hence, sequential multiscale methods are employed, which first analyze the fine scale, determine, for instance, constitutive relationships, and subsequently apply these on the coarse scale, which is addressed in a separate simulation (Tadmor & Miller, 2011).

Lau et al. (2012) study an epoxy-silica interface and employ the metadynamics (Laio & Gervasio, 2008) algorithm to construct the free energy surface of a single chain detaching from the adherend surface. By applying the obtained free energy in a worm-like-chain fracture model (Keten & Buehler, 2008), they determine Young's Modulus, maximum debonding stress, and fracture energy. These three parameters uniquely define a triangular traction-separation law, which they employ to analyze a CFRP-concrete joint using CZM. Despite the large number of assumptions and limitations they obtain good agreement with experimental results, demonstrating that an upscaling from the atomistic to the continuum scale is possible. Yang & Qu (2014a) investigate the mechanical behavior of an epoxy molding compound near a copper substrate. First, they derive the epoxy-copper interactions with a metadynamics approach (Laio & Gervasio, 2008).

Second, they observe a structural interphase region with density fluctuations reaching 2 nm from the copper surface. This structural interphase results in a larger mechanical interphase of 10 nm where bead displacements differ from the bulk material. Finally, they derive a nano-scale traction-separation law from the stress-strain response of the copper-epoxy samples, which could be used in a CZM approach. In a recent contribution, Chowdhury & Gillespie (2024) derive a traction-separation law for epoxy-silica interfaces directly from atomistic MD simulations. To this end, they apply mode I (Chowdhury & Gillespie, 2022), mode II, and mixed-mode loading at a wide range of strain rates, including a quasi-static approximation derived via stress relaxation. They utilize the MD results to calibrate a trapezoidal traction-separation law and parametrize its parameters as functions of strain rate and load angle to capture all mixed mode conditions. Hence, they bridge scales by translating their findings from the atomistic scale into an efficient continuum model.

The multiscale approaches presented above demonstrate that it is possible to homogenize fine scale MD results and reproduce them using more efficient continuum methods, such as CZM. This facilitates direct comparisons with experimental investigations, thereby helping to elucidate the structure-property relation of adhesive joints. Consequently, these multiscale methods not only connect different scales but also help bridge the gap between the experimental and simulation communities.

6. Conclusions

This contribution provides an overview of the most relevant simulation methods for studying the mechanical behavior of adhesive joints. Various techniques can be used to model these joints accurately. Particle-based approaches like molecular dynamics (MD) are limited to small time and length scales. As a result, they primarily focus on the influence of surface chemistry, the formation of the interphase, and the degradation caused by defects and moisture. In contrast, various continuum-based methods, particularly cohesive zone models (CZM), are employed to predict the macroscopic properties – such as strength and toughness – of adhesive joints. These methods successfully capture many important aspects, including temperature, strain rate, load case, moisture content, adhesive type, material pairing, and bond geometry. However, this is typically achieved by empirically adjusting the model parameters instead of considering the microstructure. To overcome this limitation, multiscale approaches have been developed to determine the parameters of CZMs through MD simulations. These methods help in understanding the multiscale

behavior of adhesive bonds. However, there is still a need for more comprehensive approaches to fully comprehend the structure-property relationships of adhesive joints from the molecular level to the macroscopic scale. Starting from precise atomistic MD, an efficient particle model capturing an adhesive layer between two substrates at molecular resolution could be obtained through coarse-graining. Using the resulting coarse-grained model, interphase properties and surface effects can be studied ultimately integrating these findings into a traction-separation law which facilitates macroscopic CZM studies. Such an upscaling methodology – from the atomistic level to the macroscale – allows us to identify the impact of molecular factors, such as surface chemistry, topology, and moisture, on the macroscopic behavior of adhesive joints.

Funding

This research was funded by the Deutsche Forschungsgemeinschaft (DFG, German Research Foundation) – 377472739/GRK2423/2-2023andFriedrich-Alexander-Universität Erlangen-Nürnberg Emerging Talent Initiative – ETI 2024-1_Tech_06_Ries.

Acknowledgement

We would like to sincerely thank Özge Akar, Lucie Spannraft, and Gunnar Possart from Friedrich-Alexander-Universität Erlangen-Nürnberg for the fruitful discussions on cohesive zone models, generalized interfaces, and adhesive joints, respectively.

References

Abdalla, A. M. A., Elmoghazy, Y. H., Sarkon, G. K., Gazioglu, A., Sabry, O. K., Sawelih, A. A., Al Sharif, A., Wehbi, H., Ali Abd, A. Y., Sahmani, S., & Safaei, B. (2025). Exploring the impact of graphene nanoplatelets on adhesive mechanical strength: A comprehensive investigation into single-lap joint elastoplastic behavior via cohesive zone method. *International Journal of Adhesion and Adhesives*, *138*, 103908. https://doi.org/10.1016/j.ijadhadh.2024.103908.

Adams, R. D., Cowap, J. W., Farquharson, G., Margary, G. M., & Vaughn, D. (2009). The relative merits of the Boeing wedge test and the double cantilever beam test for assessing the durability of adhesively bonded joints, with particular reference to the use of fracture mechanics. *International Journal of Adhesion and Adhesives*, *29*(6), 609–620. https://doi.org/10.1016/j.ijadhadh.2009.02.010.

Africa, P. C., Arndt, D., Bangerth, W., Blais, B., Fehling, M., Gassmöller, R., Heister, T., Heltai, L., Kinnewig, S., Kronbichler, M., Maier, M., Munch, P., Schreter-Fleischhacker, M., Thiele, J. P., Turcksin, B., Wells, D., & Yushutin, V. (2024). The deal.II library, version 9.6. *Journal of Numerical Mathematics*, *32*(4), 369–380. https://doi.org/10.1515/jnma-2024-0137.

Alfano, G., & Crisfield, M. A. (2001). Finite element interface models for the delamination analysis of laminated composites: Mechanical and computational issues. *International Journal for Numerical Methods in Engineering*, *50*(7), 1701–1736. https://doi.org/10.1002/nme.93.

Ali-Ahmad, M., Subramaniam, K., & Ghosn, M. (2006). Experimental investigation and fracture analysis of debonding between concrete and frp sheets. *Journal of Engineering Mechanics*, *132*(9), 914–923. https://doi.org/10.1061/(asce)0733-9399(2006)132:9(914).

Allen, M. P. (2004). Introduction to molecular dynamics simulation. In N. Attig, K. Binder, H. Grubmüller, K. Kremer (Eds.), *Computational Soft Matter: From Synthetic Polymers to Proteins. Lecture Notes*. John von Neumann Institute for Computing.

Allix, O., & Corigliano, A. (1996). Modeling and simulation of crack propagation in mixed-modes interlaminar fracture specimens. *International Journal of Fracture*, *77*, 111–140. https://doi.org/10.1007/BF00037233.

Aramoon, A., Breitzman, T. D., Woodward, Ch., & El-Awady, J. A. (2016). Coarse-grained molecular dynamics study of the curing and properties of highly cross-linked epoxy polymers. *The Journal of Physical Chemistry B*, *120*(35), 9495–9505. https://doi.org/10.1021/acs.jpcb.6b03809.

Armstrong, K. (1997). Long-term durability in water of aluminium alloy adhesive joints bonded with epoxy adhesives. *International Journal of Adhesion and Adhesives*, *17*(2), 89–105. https://doi.org/10.1016/s0143-7496(96)00038-3.

Ascione, F., & Mancusi, G. (2010). Failure criteria for FRP adhesive lap joints: A comparative analysis. *Mechanics of Advanced Materials and Structures*, *17*(2), 157–164. https://doi.org/10.1080/15376490903556659.

Aufray, M., & Roche, A. A. (2007). Epoxy–amine/metal interphases: Influences from sharp needle-like crystal formation. *International Journal of Adhesion and Adhesives*, *27*(5), 387–393. https://doi.org/10.1016/j.ijadhadh.2006.09.009.

Badulescu, C., Cognard, J. Y., Créac'hcadec, R., & Vedrine, P. (2012). Analysis of the low temperature-dependent behaviour of a ductile adhesive under monotonic tensile/compression–shear loads. *International Journal of Adhesion and Adhesives*, *36*, 56–64. https://doi.org/10.1016/j.ijadhadh.2012.03.009.

Baggioli, A., Casalegno, M., David, A., Pasquini, M., & Raos, G. (2020). Polymer-mediated adhesion: Nanoscale surface morphology and failure mechanisms. *Macromolecules*, *54*(1), 195–202. https://doi.org/10.1021/acs.macromol.0c02343.

Bandyopadhyay, A., Valavala, P. K., Clancy, T. C., Wise, K. E., & Odegard, G. M. (2011). Molecular modeling of crosslinked epoxy polymers: The effect of crosslink density on thermomechanical properties. *Polymer*, *52*(11), 2445–2452. https://doi.org/10.1016/j.polymer.2011.03.052.

Banea, M. D., Silva, L. F. M., da, & Campilho, R. D. S. G. (2010). Temperature dependence of the fracture toughness of adhesively bonded joints. *Journal of Adhesion Science and Technology*, *24*(11–12), 2011–2026. https://doi.org/10.1163/016942410x507713.

Banea, M. D., Silva, L. F. M., da, & Campilho, R. D. S. G. (2011). Mode I fracture toughness of adhesively bonded joints as a function of temperature: Experimental and numerical study. *International Journal of Adhesion and Adhesives*, *31*(5), 273–279. https://doi.org/10.1016/j.ijadhadh.2010.09.005.

Barenblatt, G. I. (1962). The mathematical theory of equilibrium cracks in brittle fracture. *Advances in Applied Mechanics*, *7*, 55–129. https://doi.org/10.1016/S0065-2156(08)70121-2.

Behera, D., Roy, P., & Madenci, E. (2021). Peridynamic modeling of bonded-lap joints with viscoelastic adhesives in the presence of finite deformation. *Computer Methods in Applied Mechanics and Engineering*, *374*, 113584. https://doi.org/10.1016/j.cma.2020.113584.

Belytschko, T., & Black, T. (1999). Elastic crack growth in finite elements with minimal remeshing. *International Journal for Numerical Methods in Engineering*, *45*(5), 601–620. https://doi.org/10.1002/(SICI)1097-0207(19990620)45:5%3C601::AID-NME598%3E3.0.CO;2-S.

Berendsen, H. J. C., Postma, J. P. M., Gunsteren, W. F., van, DiNola, A., & Haak, J. R. (1984). Molecular dynamics with coupling to an external bath. *The Journal of Chemical Physics*, *81*(8), 3684–3690. https://doi.org/10.1063/1.448118.

Bergström, J. S., & Bischoff, J. E. (2010). An advanced thermomechanical constitutive model for UHMWPE. *The International Journal of Structural Changes in Solids*, *2*(1), 31–39.

Berruet, R., Vinard, E., Calle, A., Tighzert, H., Chabert, B., Magloire, H., & Eloy, R. (1987). Mechanical properties and biocompatibility of two polyepoxy matrices: DGEBA-DDM and DGEBA-IPD. *Biomaterials*, *8*(3), 162–171. https://doi.org/10.1016/0142-9612(87)90058-5.

Bhardwaj, A., Sommer, J.-U., & Werner, M. (2024). Nucleation patterns of polymer crystals analyzed by machine learning models. *Macromolecules*, *57*(20), 9711–9724. https://doi.org/10.1021/acs.macromol.4c00920.

Blackman, B. R. K., Kinloch, A. J., Rodriguez-Sanchez, F. S., & Teo, W. S. (2012). The fracture behaviour of adhesively-bonded composite joints: Effects of rate of test and mode of loading. *International Journal of Solids and Structures*, *49*(13), 1434–1452. https://doi.org/10.1016/j.ijsolstr.2012.02.022.

Bocharova, V., Genix, A.-C., Carrillo, J.-M. Y., Kumar, R., Carroll, B., Erwin, A., Voylov, D., Kisliuk, A., Wang, Y., Sumpter, B. G., & Sokolov, A. P. (2020). Addition of short polymer chains mechanically reinforces glassy poly (2-vinylpyridine)-silica nanoparticle nanocomposites. *ACS Applied Nano Materials*, *3*(4), 3427–3438. https://doi.org/10.1021/acsanm.0c00180.

Bourdin, B., Francfort, G. A., & Marigo, J.-J. (2000). Numerical experiments in revisited brittle fracture. *Journal of the Mechanics and Physics of Solids*, *48*(4), 797–826. https://doi.org/10.1016/s0022-5096(99)00028-9.

Brooks, B. R., Bruccoleri, R. E., Olafson, B. D., States, D. J., Swaminathan, S., & Karplus, M. (1983). CHARMM: A program for macromolecular energy, minimization, and dynamics calculations. *Journal of Computational Chemistry*, *4*(2), 187–217. https://doi.org/10.1002/jcc.540040211.

Brown, D., & Clarke, J. H. R. (1991). Molecular dynamics simulation of an amorphous polymer under tension. 1. Phenomenology. *Macromolecules*, *24*(8), 2075–2082. https://doi.org/10.1021/ma00008a056.

Büyüköztürk, O., Buehler, M. J., Lau, D., & Tuakta, C. (2011). Structural solution using molecular dynamics: Fundamentals and a case study of epoxy-silica interface. *International Journal of Solids and Structures*, *48*(14–15), 2131–2140. https://doi.org/10.1016/j.ijsolstr.2011.03.018.

Cadenaro, M., Maravic, T., Comba, A., Mazzoni, A., Fanfoni, L., Hilton, T., Ferracane, J., & Breschi, L. (2019). The role of polymerization in adhesive dentistry. *Dental Materials*, *35*(1), e1–e22. https://doi.org/10.1016/j.dental.2018.11.012.

Campilho, R. D. S. G., Moura, M. F. S. F., de, & Domingues, J. J. M. S. (2008). Using a cohesive damage model to predict the tensile behaviour of CFRP single-strap repairs. *International Journal of Solids and Structures*, *45*(5), 1497–1512. https://doi.org/10.1016/j.ijsolstr.2007.10.003.

Campilho, R. D. S. G., Banea, M. D., Chaves, F. J. P., & Silva, L. F. M., da (2011a). eXtended Finite Element Method for fracture characterization of adhesive joints in pure mode I. *Computational Materials Science*, *50*(4), 1543–1549. https://doi.org/10.1016/j.commatsci.2010.12.012.

Campilho, R. D. S. G., Banea, M. D., Pinto, A. M. G., Silva, L. F. M., da, & Jesus, A. M. P., de (2011b). Strength prediction of single- and double-lap joints by standard and extended finite element modelling. *International Journal of Adhesion and Adhesives*, *31*(5), 363–372. https://doi.org/10.1016/j.ijadhadh.2010.09.008.

Campilho, R. D. S. G., Banea, M. D., Neto, J. A. B. P., & Silva, L. F. M., da (2013). Modelling adhesive joints with cohesive zone models: Effect of the cohesive law shape of the adhesive layer. *International Journal of Adhesion and Adhesives*, *44*, 48–56. https://doi.org/10.1016/j.ijadhadh.2013.02.006.

Carlberger, T., Biel, A., & Stigh, U. (2009). Influence of temperature and strain rate on cohesive properties of a structural epoxy adhesive. *International Journal of Fracture*, *155*, 155–166. https://doi.org/10.1007/s10704-009-9337-4.

Chandra, N., Li, H., Shet, C., & Ghonem, H. (2002). Some issues in the application of cohesive zone models for metal-ceramic interfaces. *International Journal of Solids and Structures*, *39*(10), 2827–2855. https://doi.org/10.1016/S0020-7683(02)00149-X.

Chang, S.-H., & Kim, H.-S. (2011). Investigation of hygroscopic properties in electronic packages using molecular dynamics simulation. *Polymer*, *52*(15), 3437–3442. https://doi.org/10.1016/j.polymer.2011.05.056.

Chaouch, S., & Yvonnet, J. (2024). Unsupervised machine learning classification for accelerating FE^2 multiscale fracture simulations. *Computer Methods in Applied Mechanics and Engineering*, *432*, 117278. https://doi.org/10.1016/j.cma.2024.117278.

Chen, J. (2002). Predicting progressive delamination of stiffened fibre-composite panel and repaired sandwich panel by decohesion models. *Journal of Thermoplastic Composite Materials*, *15*(5), 429–442. https://doi.org/10.1177/089270570201 5005736.

Chiang, M. Y. M., & Fernandez-Garcia, M. (2002). Relation of swelling and T_g depression to the apparent free volume of a particle-filled, epoxy-based adhesive. *Journal of Applied Polymer Science*, *87*(9), 1436–1444. https://doi.org/10.1002/app.11576.

Chowdhury, S. C., & Gillespie, J. W. (2022). Strain-rate dependent mode i cohesive traction laws for glass fiber-epoxy interphase using molecular dynamics simulations. *Composites Part B: Engineering*, *237*, 109877. https://doi.org/10.1016/j.compositesb.2022.109877.

Chowdhury, S. C., & Gillespie, J. W. (2024). Strain-rate dependent mixed-mode traction laws for glass fiber-epoxy interphase using molecular dynamics simulations. *Composites Part B: Engineering*, *275*, 111351. https://doi.org/10.1016/j.compositesb.2024.111351.

Clancy, T. C., Frankland, S. J. V., Hinkley, J. A., & Gates, T. S. (2009). Molecular modeling for calculation of mechanical properties of epoxies with moisture ingress. *Polymer*, *50*(12), 2736–2742. https://doi.org/10.1016/j.polymer.2009.04.021.

De Carvalho, N. V., Mabson, G. E., Krueger, R., & Deobald, L. R. (2019). A new approach to model delamination growth in fatigue using the virtual crack closure technique without re-meshing. *Engineering Fracture Mechanics*, *222*, 106614. https://doi.org/10.1016/j.engfracmech.2019.106614.

De Nograro, F. F., Guerrero, P., Corcuera, M. A., & Mondragon, I. (1995). Effects of chemical structure of hardener on curing evolution and on the dynamic mechanical behavior of epoxy resins. *Journal of Applied Polymer Science*, *56*(2), 177–192. https://doi.org/10.1002/app.1995.070560208.

Deng, J., Song, Y., Lan, Z., Xu, Z., Chen, Y., Yang, B., & Hao, H. (2022). The surface modification effect on the interfacial properties of glass fiber-reinforced epoxy: A molecular dynamics study. *Nanotechnology Reviews*, *11*(1), 1143–1157. https://doi.org/10.1515/ntrev-2022-0068.

Dietz, J. D., Nan, K., & Hoy, R. S. (2022). Unexpected ductility in semiflexible polymer glasses with entanglement length equal to their Kuhn length. *Physical Review Letters*, *129*(12), 127801. https://doi.org/10.1103/PhysRevLett.129.127801.

Dorduncu, M. (2020). Peridynamic modeling of adhesively bonded beams with modulus graded adhesives using refined zigzag theory. *International Journal of Mechanical Sciences*, *185*, 105866. https://doi.org/10.1016/j.ijmecsci.2020.105866.

Dugdale, D. S. (1960). Yielding of steel sheets containing slits. *Journal of the Mechanics and Physics of Solids*, *8*(2), 100–104. https://doi.org/10.1016/0022-5096(60)90013-2.

Duin, A. C. T., van, Dasgupta, S., Lorant, F., & Goddard, W. A. (2001). ReaxFF: A reactive force field for hydrocarbons. *The Journal of Physical Chemistry A*, *105*(41), 9396–9409. https://doi.org/10.1021/jp004368u.

Esmaeili, A., Steinmann, P., & Javili, A. (2017). Non-coherent energetic interfaces accounting for degradation. *Computational Mechanics*, *59*, 361–383. https://doi.org/10.1007/s00466-016-1342-7.

Español, P., & Warren, P. (1995). Statistical mechanics of dissipative particle dynamics. *Europhysics Letters*, *30*(4), 191. https://doi.org/10.1209/0295-5075/30/4/001.

Evans, D. J., & Holian, B. L. (1985). The Nose–Hoover thermostat. *The Journal of Chemical Physics*, *83*(8), 4069–4074. https://doi.org/10.1063/1.449071.

Everaers, R., Karimi-Varzaneh, H. A., Fleck, F., Hojdis, N., & Svaneborg, C. (2020). Kremer–grest models for commodity polymer melts: Linking theory, experiment, and simulation at the Kuhn scale. *Macromolecules*, *53*(6), 1901–1916. https://doi.org/10.1021/acs.macromol.9b02428.

Faller, R., Kolb, A., & Müller-Plathe, F. (1999). Local chain ordering in amorphous polymer melts: Influence of chain stiffness. *Physical Chemistry Chemical Physics*, *1*(9), 2071–2076. https://doi.org/10.1039/A809796H.

Fata, D., Bockenheimer, C., & Possart, W. (2005). Chapter 30. Epoxies on stainless steel-curing and aging. In W. Possart (Ed.), *Adhesion: Current Research and Application* (pp. 479–506). Wiley-VCH. https://doi.org/10.1002/3527607307.

Fernandes, T. A. B., Campilho, R. D. S. G., Banea, M. D., & Silva, L. F. M., da (2015). Adhesive selection for single lap bonded joints: Experimentation and advanced techniques for strength prediction. *The Journal of Adhesion*, *91*(10–11), 841–862. https://doi.org/10.1080/00218464.2014.994703.

Feyel, F. (1999). Multiscale FE^2 elastoviscoplastic analysis of composite structures. *Computational Materials Science*, *16*(1–4), 344–354. https://doi.org/10.1016/S0927-0256(99)00077-4.

Firooz, S., & Javili, A. (2019). Understanding the role of general interfaces in the overall behavior of composites and size effects. *Computational Materials Science*, *162*, 245–254. https://doi.org/10.1016/j.commatsci.2019.02.042.

Floros, I. S., Tserpes, K. I., & Löbel, T. (2015). Mode-I, mode-II and mixed-mode I+II fracture behavior of composite bonded joints: Experimental characterization and numerical simulation. *Composites Part B: Engineering*, *78*, 459–468. https://doi.org/10.1016/j.compositesb.2015.04.006.

Frenkel, D., & Smit, B. (2023). *Understanding Molecular Simulation: From Algorithms to Applications* (3rd ed.). Elsevier.

Fritz, D., Koschke, K., Harmandaris, V. A., Vegt, N. F. A., van der, & Kremer, K. (2011). Multiscale modeling of soft matter: Scaling of dynamics. *Physical Chemistry Chemical Physics*, *13*(22), 10412. https://doi.org/10.1039/c1cp20247b.

Garcia, F. G., Soares, B. G., Pita, V. J. R. R., Sánchez, R., & Rieumont, J. (2007). Mechanical properties of epoxy networks based on DGEBA and aliphatic amines. *Journal of Applied Polymer Science*, *106*(3), 2047–2055. https://doi.org/10.1002/app.24895.

Gavrilov, A. A., Komarov, P. V., & Khalatur, P. G. (2014). Thermal properties and topology of epoxy networks: A multiscale simulation methodology. *Macromolecules*, *48*(1), 206–212. https://doi.org/10.1021/ma502220k.

Ghareeb, A., & Elbanna, A. (2020). An adaptive quasicontinuum approach for modeling fracture in networked materials: Application to modeling of polymer networks. *Journal of the Mechanics and Physics of Solids*, *137*, 103819. https://doi.org/10.1016/j.jmps.2019.103819.

Giuntoli, A., Hansoge, N. K., Beek, A., van, Meng, Z., Chen, W., & Keten, S. (2021). Systematic coarse-graining of epoxy resins with machine learning-informed energy renormalization. *npj Computational Materials*, *7*(1), 168. https://doi.org/10.1038/s41524-021-00634-1.

González, M. (2011). Force fields and molecular dynamics simulations. *JDN*, *12*, 169–200. https://doi.org/10.1051/sfn/201112009.

Griffith, A. A. (1921). VI. The phenomena of rupture and flow in solids. *Philosophical Transactions of the Royal Society A*, *221*(582–593), 163–198. https://doi.org/10.1098/rsta.1921.0006.

Groot, R. D., & Warren, P. B. (1997). Dissipative particle dynamics: Bridging the gap between atomistic and mesoscopic simulation. *The Journal of Chemical Physics*, *107*(11), 4423–4435. https://doi.org/10.1063/1.474784.

Gusev, A. A., Zehnder, M. M., & Suter, U. W. (1996). Fluctuation formula for elastic constants. *Physical Review B*, *54*(1). https://doi.org/10.1103/PhysRevB.54.1.

Haba, D., Brunner, A. J., Barbezat, M., Spetter, D., Tremel, W., & Pinter, G. (2016). Correlation of epoxy material properties with the toughening effect of fullerene-like WS_2 nanoparticles. *European Polymer Journal*, *84*, 125–136. https://doi.org/10.1016/j.eurpolymj.2016.09.022.

Han, X., Crocombe, A. D., Anwar, S. N. R., & Hu, P. (2014). The strength prediction of adhesive single lap joints exposed to long term loading in a hostile environment. *International Journal of Adhesion and Adhesives*, *55*, 1–11. https://doi.org/10.1016/j.ijadhadh.2014.06.013.

Hasheminia, S. M., Park, B. Ch., Chun, H.-J., Park, J.-Ch., & Chang, H. S. (2019). Failure mechanism of bonded joints with similar and dissimilar material. *Composites Part B: Engineering*, *161*, 702–709. https://doi.org/10.1016/j.compositesb.2018.11.016.

Häßler, R., & Mühlen, E., zur (2000). An introduction to μta and its application to the study of interfaces. *Thermochimica Acta*, *361*(1–2), 113–120. https://doi.org/10.1016/s0040-6031(00)00552-9.

Hiemenz, P. C., & Lodge, T. P. (2007). *Polymer Chemistry* (2nd ed.). CRC Press. https://doi.org/10.1201/9781420018271.

Hillerborg, A., Modéer, M., & Petersson, P.-E. (1976). Analysis of crack formation and crack growth in concrete by means of fracture mechanics and finite elements. *Cement and Concrete Research*, *6*(6), 773–781. https://doi.org/10.1016/0008-8846(76)90007-7.

Holzapfel, G. A. (2000). *Nonlinear Solid Mechanics: A Continuum Approach for Engineering Science*. Wiley.

Hutchinson, J. W., & Suo, Z. (1991). Mixed mode cracking in layered materials. In J. W. Hutchinson, T. Y. Wu (Eds.), *Advances in Applied Mechanics* (vol. 29, pp. 63–191). Elsevier. https://doi.org/10.1016/s0065-2156(08)70164-9.

Izrailev, S., Stepaniants, S., Isralewitz, B., Kosztin, D., Lu, H., Molnar, F., Wriggers, W., & Schulten, K. (1999). Steered molecular dynamics. In P. Deuflhard, J. Hermans, B. Leimkuhler, A. E. Mark, S. Reich, R. D. Skeel (Eds.), *Computational molecular dynamics: Challenges, methods, ideas* (pp. 39–65). Springer Berlin Heidelberg. https://doi.org/10.1007/978-3-642-58360-5_2.

Jahani, Y., Baena, M., Barris, C., Perera, R., & Torres, L. (2022). Influence of curing, post-curing and testing temperatures on mechanical properties of a structural adhesive. *Construction and Building Materials*, *324*, 126698. https://doi.org/10.1016/j.conbuildmat.2022.126698.

Jaillon, A., Jumel, J., Paroissien, E., & Lachaud, F. (2019). Mode I cohesive zone model parameters identification and comparison of measurement techniques for robustness to the law shape evaluation. *The Journal of Adhesion*, *96*(1–4), 272–299. https://doi.org/10.1080/00218464.2019.1669450.

Jang, C. W., Mullinax, J. W., & Lawson, J. W. (2022). Mechanical properties and failure of aerospace-grade epoxy resins from reactive molecular dynamics simulations with nanoscale defects. *ACS Applied Polymer Materials*, *4*(8), 5269–5274. https://doi.org/10.1021/acsapm.2c00503.

Javili, A., McBride, A. T., & Steinmann, P. (2019). Continuum-kinematics-inspired peridynamics. Mechanical problems. *Journal of the Mechanics and Physics of Solids*, *131*, 125–146. https://doi.org/10.1016/j.jmps.2019.06.016.

Jeyranpour, F., Alahyarizadeh, G., & Arab, B. (2015). Comparative investigation of thermal and mechanical properties of cross-linked epoxy polymers with different curing agents by molecular dynamics simulation. *Journal of Molecular Graphics and Modelling*, *62*, 157–164. https://doi.org/10.1016/j.jmgm.2015.09.012.

Ji, G., Ouyang, Z., Li, G., Ibekwe, S., & Pang, S.-S. (2010). Effects of adhesive thickness on global and local Mode-I interfacial fracture of bonded joints. *International Journal of Solids and Structures*, *47*(18–19), 2445–2458. https://doi.org/10.1016/j.ijsolstr.2010.05.006.

Jia, Z., Yuan, G., Hui, D., Feng, X., & Zou, Y. (2018). Effect of high loading rate and low temperature on mode i fracture toughness of ductile polyurethane adhesive. *Journal of Adhesion Science and Technology*, *33*(1), 79–92. https://doi.org/10.1080/01694243.2018.1546364.

Jin, F.-L., Li, X., & Park, S.-J. (2015). Synthesis and application of epoxy resins: A review. *Journal of Industrial and Engineering Chemistry*, *29*, 1–11. https://doi.org/10.1016/j.jiec.2015.03.026.

Jin, K., López Barreiro, D., Martin-Martinez, F. J., Qin, Z., Hamm, M., Paul, Ch. W., & Buehler, M. J. (2018). Improving the performance of pressure sensitive adhesives by tuning the crosslinking density and locations. *Polymer*, *154*, 164–171. https://doi.org/10.1016/j.polymer.2018.08.065.

Jokinen, J., Wallin, M., & Saarela, O. (2015). Applicability of VCCT in mode I loading of yielding adhesively bonded joints – a case study. *International Journal of Adhesion and Adhesives*, *62*, 85–91. https://doi.org/10.1016/j.ijadhadh.2015.07.004.

Joshi, S. Y., & Deshmukh, S. A. (2021). A review of advancements in coarse-grained molecular dynamics simulations. *Molecular Simulation*, *47*(10–11), 786–803. https://doi.org/10.1080/08927022.2020.1828583.

Kacar, G., Peters, E. A. J. F., & With, G., de (2013). Mesoscopic simulations for the molecular and network structure of a thermoset polymer. *Soft Matter*, *9*(24), 5785. https://doi.org/10.1039/c3sm50304f.

Kaczmarczyk, Ł., Ullah, Z., Lewandowski, K., Meng, X., Zhou, X.-Y., Athanasiadis, I., Nguyen, H., Chalons-Mouriesse, C.-A., Richardson, E., Miur, E., Shvarts, A., Wakeni, M., & Pearce, C. (2020). MoFEM: an open source, parallel finite element library. *The Journal of Open Source Software*, *5*(45), 1441. https://doi.org/10.21105/joss.01441.

Kanamori, K., Kimoto, Y., Toriumi, S., & Yonezu, A. (2021). On the cyclic fatigue of adhesively bonded aluminium: Experiments and molecular dynamics simulation. *International Journal of Adhesion and Adhesives*, *107*, 102848. https://doi.org/10.1016/j.ijadhadh.2021.102848.

Kanzow, J., Faupel, F., Egger, W., Sperr, P., Kögel, G., Wehlack, C., Meiser, A., & Possart, W. (2005). Chapter 29. Depth-resolved analysis of the aging behavior of epoxy thin films by positron spectroscopy. In W. Possart (Ed.), *Adhesion: Current Research and Application* (pp. 465–477). Wiley-VCH. https://doi.org/10.1002/3527607307.ch29.

Karac, A., Blackman, B. R. K., Cooper, V., Kinloch, A. J., Rodriguez Sanchez, S., Teo, W. S., & Ivankovic, A. (2011). Modelling the fracture behaviour of adhesively-bonded joints as a function of test rate. *Engineering Fracture Mechanics*, *78*(6), 973–989. https://doi.org/10.1016/j.engfracmech.2010.11.014.

Karachalios, E. F., Adams, R. D., & Silva, L. F. M., da (2013). Single lap joints loaded in tension with ductile steel adherends. *International Journal of Adhesion and Adhesives*, *43*, 96–108. https://doi.org/10.1016/j.ijadhadh.2013.01.017.

Karimi-Varzaneh, H. A., Vegt, N. F. A., van der, Müller-Plathe, F., & Carbone, P. (2012). How good are coarse-grained polymer models? A comparison for atactic polystyrene. *ChemPhysChem*, *13*(15), 3428–3439. https://doi.org/10.1002/cphc.201200111.

Katnam, K. B., Sargent, J. P., Crocombe, A. D., Khoramishad, H., & Ashcroft, I. A. (2010). Characterisation of moisture-dependent cohesive zone properties for adhesively bonded joints. *Engineering Fracture Mechanics*, *77*(16), 3105–3119. https://doi.org/10.1016/j.engfracmech.2010.08.023.

Keten, S., & Buehler, M. J. (2008). Asymptotic strength limit of hydrogen-bond assemblies in proteins at vanishing pulling rates. *Physical Review Letters*, *100*(19). https://doi.org/10.1103/physrevlett.100.198301.

Khoramishad, H., Crocombe, A. D., Katnam, K. B., & Ashcroft, I. A. (2010). Predicting fatigue damage in adhesively bonded joints using a cohesive zone model. *International Journal of Fatigue*, *32*(7), 1146–1158. https://doi.org/10.1016/j.ijfatigue.2009.12.013.

Konrad, J., & Zahn, D. (2023). Interfaces in reinforced epoxy resins: From molecular scale understanding towards mechanical properties. *Journal of Molecular Modeling*, *29*(8), 243. https://doi.org/10.1007/s00894-023-05654-w.

Konrad, J., Meißner, R. H., Bitzek, E., & Zahn, D. (2021). A molecular simulation approach to bond reorganization in epoxy resins: From curing to deformation and fracture. *ACS Polymers Au*, *1*(3), 165–174. https://doi.org/10.1021/acspolymersau.1c00016.

Kremer, K., & Grest, G. S. (1990). Dynamics of entangled linear polymer melts: A molecular-dynamics simulation. *The Journal of Chemical Physics*, *92*(8), 5057–5086. https://doi.org/10.1063/1.458541.

Kröger, M. (2004). Simple models for complex nonequilibrium fluids. *Physics Reports*, *390*(6), 453–551. https://doi.org/10.1016/j.physrep.2003.10.014.

Kröger, M., Dietz, J. D., Hoy, R. S., & Luap, C. (2023). The Z1+ package: Shortest multiple disconnected path for the analysis of entanglements in macromolecular systems. *Computer Physics Communications*, *283*, 108567. https://doi.org/10.1016/j.cpc.2022.108567.

Krueger, R. (2015). 1 – The virtual crack closure technique for modeling interlaminar failure and delamination in advanced composite materials. In P. P. Camanho, S. R. Hallett (Eds.), *Numerical Modelling of Failure in Advanced Composite Materials* (pp. 3–53). Elsevier. https://doi.org/10.1016/b978-0-08-100332-9.00001-3.

Laio, A., & Gervasio, F. L. (2008). Metadynamics: A method to simulate rare events and reconstruct the free energy in biophysics, chemistry and material science. *Reports on Progress in Physics*, *71*(12), 126601. https://doi.org/10.1088/0034-4885/71/12/126601.

Langeloth, M., Sugii, T., Böhm, M. C., & Müller-Plathe, F. (2015). The glass transition in cured epoxy thermosets: A comparative molecular dynamics study in coarse-grained and atomistic resolution. *The Journal of Chemical Physics*, *143*(24), 243158. https://doi.org/10.1063/1.4937627.

Lapique, F., & Redford, K. (2002). Curing effects on viscosity and mechanical properties of a commercial epoxy resin adhesive. *International Journal of Adhesion and Adhesives*, *22*(4), 337–346. https://doi.org/10.1016/s0143-7496(02)00013-1.

Lau, D., Büyüköztürk, O., & Buehler, M. J. (2012). Characterization of the intrinsic strength between epoxy and silica using a multiscale approach. *Journal of Materials Research*, *27*(14), 1787–1796. https://doi.org/10.1557/jmr.2012.96.

Laurien, M., Javili, A., & Steinmann, P. (2023). Peridynamic modeling of nonlocal degrading interfaces in composites. *Forces in Mechanics*, *10*, 100124. https://doi.org/10.1016/j.finmec.2022.100124.

Laurien, M., Javili, A., & Steinmann, P. (2024). Nonlocal interfaces accounting for progressive damage within continuum-kinematics-inspired peridynamics. *International Journal of Solids and Structures*, *290*, 112641. https://doi.org/10.1016/j.ijsolstr.2023.112641.

Li, Ch., & Strachan, A. (2016). Free volume evolution in the process of epoxy curing and its effect on mechanical properties. *Polymer*, *97*, 456–464. https://doi.org/10.1016/j.polymer.2016.05.059.

Li, Ch., Ke, L., He, J., Chen, Z., & Jiao, Y. (2019). Effects of mechanical properties of adhesive and CFRP on the bond behavior in CFRP-strengthened steel structures. *Composite Structures*, *211*, 163–174. https://doi.org/10.1016/j.compstruct.2018.12.020.

Li, K., Li, Y., Lian, Q., Cheng, J., & Zhang, J. (2016a). Influence of cross-linking density on the structure and properties of the interphase within supported ultrathin epoxy films. *Journal of Materials Science*, *51*(19), 9019–9030. https://doi.org/10.1007/s10853-016-0155-6.

Li, K., Huo, N., Liu, X., Cheng, J., & Zhang, J. (2016b). Effects of the furan ring in epoxy resin on the thermomechanical properties of highly cross-linked epoxy networks: A molecular simulation study. *RSC Advances*, *6*(1), 769–777. https://doi.org/10.1039/C5RA22955C.

Li, M., Gu, Y.-Z., Liu, H., Li, Y.-X., Wang, S.-K., Wu, Q., & Zhang, Z.-G. (2013). Investigation the interphase formation process of carbon fiber/epoxy composites using a multiscale simulation method. *Composites Science and Technology*, *86*, 117–121. https://doi.org/10.1016/j.compscitech.2013.07.008.

Li, P., Li, W., Li, B., Yang, S., Shen, Y., Wang, Q., & Zhou, K. (2023). A review on phase field models for fracture and fatigue. *Engineering Fracture Mechanics*, *289*, 109419. https://doi.org/10.1016/j.engfracmech.2023.109419.

Liao, L., Huang, C., & Sawa, T. (2013). Effect of adhesive thickness, adhesive type and scarf angle on the mechanical properties of scarf adhesive joints. *International Journal of Solids and Structures*, *50*(25–26), 4333–4340. https://doi.org/10.1016/j.ijsolstr.2013.09.005.

Lin, K., & Wang, Z. (2023). Multiscale mechanics and molecular dynamics simulations of the durability of fiber-reinforced polymer composites. *Communications Materials*, *4*(1), 66. https://doi.org/10.1038/s43246-023-00391-2.

Liu, H., Uhlherr, A., Varley, R. J., & Bannister, M. K. (2004). Influence of substituents on the kinetics of epoxy/aromatic diamine resin systems. *Journal of Polymer Science Part A: Polymer Chemistry*, *42*(13), 3143–3156. https://doi.org/10.1002/pola.20169.

Livraghi, M., Höllring, K., Wick, Ch. R., Smith, D. M., & Smith, A.-S. (2021). An exact algorithm to detect the percolation transition in molecular dynamics simulations of cross-linking polymer networks. *Journal of Chemical Theory and Computation*, *17*(10), 6449–6457. https://doi.org/10.1021/acs.jctc.1c00423.

Livraghi, M., Pahi, S., Nowakowski, P., Smith, D. M., Wick, Ch. R., & Smith, A.-S. (2023). Block chemistry for accurate modeling of epoxy resins. *The Journal of Physical Chemistry B*, *127*(35), 7648–7662. https://doi.org/10.1021/acs.jpcb.3c04724.

Loh, W. K., Crocombe, A. D., Abdel Wahab, M. M., & Ashcroft, I. A. (2002). Environmental degradation of the interfacial fracture energy in an adhesively bonded joint. *Engineering Fracture Mechanics*, *69*(18), 2113–2128. https://doi.org/10.1016/s0013-7944(02)00004-8.

Lu, X., Giovanis, D. G., Yvonnet, J., Papadopoulos, V., Detrez, F., & Bai, J. (2018). A data-driven computational homogenization method based on neural networks for the nonlinear anisotropic electrical response of graphene/polymer nanocomposites. *Computational Mechanics*, *64*(2), 307–321. https://doi.org/10.1007/s00466-018-1643-0.

Ma, Q., Huang, D., Wu, L., & Xu, Y. (2023). An extended peridynamic model for analyzing interfacial failure of composite materials with non-uniform discretization. *Theoretical and Applied Fracture Mechanics*, *125*, 103854. https://doi.org/10.1016/j.tafmec.2023.103854.

Maguire, J. F., Talley, P. L., & Lupkowski, M. (1994). The interphase in adhesion: Bridging the gap. *The Journal of Adhesion*, *45*(1–4), 269–290. http://doi.org/10.1080/00218469408026643.

Mancusi, G., & Ascione, F. (2013). Performance at collapse of adhesive bonding. *Composite Structures*, *96*, 256–261. https://doi.org/10.1016/j.compstruct.2012.09.027.

Maple, J. R., Hwang, M.-J., Stockfisch, T. P., Dinur, U., Waldman, M., Ewig, C. S., & Hagler, A. T. (1994). Derivation of class II force fields. I. Methodology and quantum force field for the alkyl functional group and alkane molecules. *Journal of Computational Chemistry*, *15*(2), 162–182. https://doi.org/10.1002/jcc.540150207.

Marques, E. A. S., Silva, L. F. M., da, Banea, M. D., & Carbas, R. J. C. (2014). Adhesive joints for low- and high-temperature use: An overview. *The Journal of Adhesion*, *91*(7), 556–585. https://doi.org/10.1080/00218464.2014.943395.

Martyna, G. J., Tobias, D. J., & Klein, M. L. (1994). Constant pressure molecular dynamics algorithms. *The Journal of Chemical Physics*, *101*(5), 4177–4189. https://doi.org/10.1063/1.467468.

Mayo, S. L., Olafson, B. D., & Goddard, W. A. (1990). Dreiding: A generic force field for molecular simulations. *The Journal of Physical Chemistry*, *94*(26), 8897–8909. https://doi.org/10.1021/j100389a010.

Meiser, A., & Possart, W. (2011). Epoxy-metal interphases: Chemical and mechanical aging. *The Journal of Adhesion*, *87*(4), 313–330. https://doi.org/10.1080/00218464.2011.562105.

Meiser, A., Willstrand, K., Fehling, P., & Possart, W. (2008). Chemical aging in epoxies: A local study of the interphases to air and to metals. *The Journal of Adhesion*, *84*(4), 299–321. https://doi.org/10.1080/00218460802004360.

Meiser, A., Kübel, C., Schäfer, H., & Possart, W. (2010). Electron microscopic studies on the diffusion of metal ions in epoxy-metal interphases. *International Journal of Adhesion and Adhesives*, *30*(3), 170–177. https://doi.org/10.1016/j.ijadhadh.2009.12.001.

Meng, L., Zhang, H., Liu, Z., Shu, X., & Li, P. (2024). A direct FE^2 method for concurrent multilevel modeling of a coupled thermoelectric problem – Joule heating effect – in multiscale materials and structures. *Thin-Walled Structures*, *203*, 112166. https://doi.org/10.1016/j.tws.2024.112166.

Mészáros, L., Horváth, A., Vas, L. M., & Petrény, R. (2023). Investigation of the correlations between the microstructure and the tensile properties multi-scale composites with a polylactic acid matrix, reinforced with carbon nanotubes and carbon fibers, with the use of the fiber bundle cell theory. *Composites Science and Technology*, *242*, 110154. https://doi.org/10.1016/j.compscitech.2023.110154.

Miehe, C., Welschinger, F., & Hofacker, M. (2010). Thermodynamically consistent phase-field models of fracture: Variational principles and multi-field fe implementations. *International Journal for Numerical Methods in Engineering*, *83*(10), 1273–1311. https://doi.org/10.1002/nme.2861.

Min, K., Rammohan, A. R., Lee, H. S., Shin, J., Lee, S. H., Goyal, S., Park, H., Mauro, J. C., Stewart, R., Botu, V., Kim, H., & Cho, E. (2017). Computational approaches for investigating interfacial adhesion phenomena of polyimide on silica glass. *Scientific Reports*, *7*(1), 10475. https://doi.org/10.1038/s41598-017-10994-8.

Moës, N., Dolbow, J., & Belytschko, T. (1999). A finite element method for crack growth without remeshing. *International Journal for Numerical Methods in Engineering*, *46*(1), 131–150. https://doi.org/10.1002/(SICI)1097-0207(19990910)46:1<131::AID-NME726>3.0.CO;2-J.

Moghimikheirabadi, A., Karatrantos, A. V., & Kröger, M. (2021). Ionic polymer nanocomposites subjected to uniaxial extension: A nonequilibrium molecular dynamics study. *Polymers*, *13*(22), 4001. https://doi.org/10.3390/polym13224001.

Mohapatra, P. C., & Smith, L. V. (2019). Characterization of adhesive yield criteria usingmixed-mode loading. *Journal of Adhesion Science and Technology*, *33*(11), 1248–1260. https://doi.org/10.1080/01694243.2019.1585058.

Moya-Sanz, E. M., Ivañez, I., & Garcia-Castillo, S. K. (2017). Effect of the geometry in the strength of single-lap adhesive joints of composite laminates under uniaxial tensile load. *International Journal of Adhesion and Adhesives*, *72*, 23–29. https://doi.org/10.1016/j.ijadhadh.2016.10.009.

Nemati Giv, A., Ayatollahi, M. R., Ghaffari, S. H., & Silva, L. F., da (2018). Effect of reinforcements at different scales on mechanical properties of epoxy adhesives and adhesive joints: A review. *The Journal of Adhesion*, *94*(13), 1082–1121. https://doi.org/10.1080/00218464.2018.1452736.

Neto, J. A. B. P., Campilho, R. D. S. G., & Silva, L. F. M., da (2012). Parametric study of adhesive joints with composites. *International Journal of Adhesion and Adhesives*, *37*, 96–101. https://doi.org/10.1016/j.ijadhadh.2012.01.019.

Noid, W. G., Chu, J.-W., Ayton, G. S., Krishna, V., Izvekov, S., Voth, G. A., Das, A., & Andersen, H. C. (2008a). The multiscale coarse-graining method. I. A rigorous bridge between atomistic and coarse-grained models. *The Journal of Chemical Physics*, *128*(24), 244114. https://doi.org/10.1063/1.2938860.

Noid, W. G., Liu, P., Wang, Y., Chu, J.-W., Ayton, G. S., Izvekov, S., Andersen, H. C., & Voth, G. A. (2008b). The multiscale coarse-graining method. II. Numerical implementation for coarse-grained molecular models. *The Journal of Chemical Physics*, *128*(24), 244115. https://doi.org/10.1063/1.2938857.

Nunes, S. L. S., Campilho, R. D. S. G., Silva, F. J. G., da, Sousa, C. C. R. G., de, Fernandes, T. A. B., Banea, M. D., & Silva, L. F. M., da (2015). Comparative failure assessment of single and double lap joints with varying adhesive systems. *The Journal of Adhesion*, *92*(7–9), 610–634. https://doi.org/10.1080/00218464.2015.1103227.

Pal, S., Dansuk, K., Giuntoli, A., Sirk, T. W., & Keten, S. (2023). Predicting the effect of hardener composition on the mechanical and fracture properties of epoxy resins using molecular modeling. *Macromolecules*, *56*(12), 4447–4456. https://doi.org/10.1021/acs.macromol.2c02577.

Park, H., & Cho, M. (2020). A multiscale framework for the elasto-plastic constitutive equations of crosslinked epoxy polymers considering the effects of temperature, strain rate, hydrostatic pressure, and crosslinking density. *Journal of the Mechanics and Physics of Solids*, *142*, 103962. https://doi.org/10.1016/j.jmps.2020.103962.

Park, H., Choi, J., Kim, B., Yang, S., Shin, H., & Cho, M. (2018). Toward the constitutive modeling of epoxy matrix: Temperature-accelerated quasi-static molecular simulations consistent with the experimental test. *Composites Part B: Engineering*, *142*, 131–141. https://doi.org/10.1016/j.compositesb.2018.01.018.

Parrinello, M., & Rahman, A. (1982). Strain fluctuations and elastic constants. *The Journal of Chemical Physics*, *76*(5), 2662–2666. https://doi.org/10.1063/1.443248.

Passlack, S., Brodyanski, A., Bock, W., Kopnarski, M., Presser, M., Geiß, P. L., Possart, G., & Steinmann, P. (2009). Chemical and structural characterisation of DGEBA-based epoxies by time of flight secondary ion mass spectrometry (ToF-SIMS) as a preliminary to polymer interphase characterisation. *Analytical and Bioanalytical Chemistry*, *393*(8), 1879–1888. https://doi.org/10.1007/s00216-009-2639-6.

Pfaller, S. (2022). *Discrete and continuous methods for modelling and simulation of polymer materials* [Habilitation thesis, Friedrich-Alexander-Universität Erlangen-Nürnberg]. OPEN FAU. https://doi.org/10.25593/OPUS4-FAU-18036.

Plimpton, S. (1995). Fast parallel algorithms for short-range molecular dynamics. *Journal of Computational Physics*, *117*(1), 1–19. https://doi.org/10.1006/jcph.1995.1039.

Pocius, A. V. (2012). *Adhesion and Adhesives Technology: An Introduction*. Hanser Publications.

Possart, G. (2014). *Mechanical Interphases in Adhesives: Experiments, Modelling and Simulation* [Doctoral thesis, Friedrich-Alexander-Universität Erlangen-Nürnberg].

Possart, G., Presser, M., Passlack, S., Geiß, P. L., Kopnarski, M., Brodyanski, A., & Steinmann, P. (2009). Micro-macro characterisation of DGEBA-based epoxies as a preliminary to polymer interphase modelling. *International Journal of Adhesion and Adhesives*, *29*(5), 478–487. https://doi.org/10.1016/j.ijadhadh.2008.10.001.

Possart, W., Krüger, J. K., Wehlack, C., Müller, U., Petersen, Ch., Bactavatchalou, R., & Meiser, A. (2006). Formation and structure of epoxy network interphases at the contact to native metal surfaces. *Comptes Rendus. Chimie*, *9*(1), 60–79. https://doi.org/10.1016/j.crci.2005.04.009.

Pramanik, A., Basak, A. K., Dong, Y., Sarker, P. K., Uddin, M. S., Littlefair, G., Dixit, A. R., & Chattopadhyaya, S. (2017). Joining of carbon fibre reinforced polymer (CFRP) composites and aluminium alloys – a review. *Composites Part A: Applied Science and Manufacturing*, *101*, 1–29. https://doi.org/10.1016/j.compositesa.2017.06.007.

Qi, B., Zhang, Q. X., Bannister, M., & Mai, Y.-W. (2006). Investigation of the mechanical properties of DGEBA-based epoxy resin with nanoclay additives. *Composite Structures*, *75*(1–4), 514–519. https://doi.org/10.1016/j.compstruct.2006.04.032.

Raghava, R., Caddell, R. M., & Yeh, G. S. Y. (1973). The macroscopic yield behaviour of polymers. *Journal of Materials Science*, *8*, 225–232. https://doi.org/10.1007/BF00550671.

Ramalho, L. D. C., Sánchez-Arce, I. J., Gonçalves, D. C., Belinha, J., & Campilho, R. D. S. G. (2022). Numerical analysis of the dynamic behaviour of adhesive joints: A review. *International Journal of Adhesion and Adhesives*, *118*, 103219. https://doi.org/10.1016/j.ijadhadh.2022.103219.

Raos, G., & Zappone, B. (2024). Tuning adhesion and energy dissipation in polymer films between solid surfaces via grafting and cross-linking. *Macromolecules*, *57*(14), 6502–6513. https://doi.org/10.1021/acs.macromol.4c00062.

Reith, D., Pütz, M., & Müller-Plathe, F. (2003). Deriving effective mesoscale potentials from atomistic simulations. *Journal of Computational Chemistry*, *24*(13), 1624–1636. https://doi.org/10.1002/jcc.10307.

Ribeiro, T. E. A., Campilho, R. D. S. G., Silva, L. F. M., da & Goglio, L. (2016). Damage analysis of composite-aluminium adhesively-bonded single-lap joints. *Composite Structures*, *136*, 25–33. https://doi.org/10.1016/j.compstruct.2015.09.054.

Ries, M. (2023). *Characterization and Modeling of Polymer Nanocomposites Across the Scales – A Comprehensive Approach Covering the Mechanical Behavior of Matrix, Filler, and Interphase* [Doctoral thesis, Friedrich-Alexander-Universität Erlangen-Nürnberg]. OPEN FAU. https://doi.org/10.25593/opus4-fau-23638.

Ries, M., Possart, G., Steinmann, P., & Pfaller, S. (2021). A coupled MD-FE methodology to characterize mechanical interphases in polymeric nanocomposites. *International Journal of Mechanical Sciences*, *204*, 106564. https://doi.org/10.1016/j.ijmecsci.2021.106564.

Ries, M., Seibert, J., Steinmann, P., & Pfaller, S. (2022). Applying a generic and fast coarse-grained molecular dynamics model to extensively study the mechanical behavior of polymer nanocomposites. *Express Polymer Letters*, *16*(12), 1304–1321. https://doi.org/10.3144/expresspolymlett.2022.94.

Ritter, J., Shegufta, S., & Zaiser, M. (2023). Effects of disorder on deformation and failure of brittle porous materials. *Journal of Statistical Mechanics: Theory and Experiment*, *2023*(5), 053301. https://doi.org/10.1088/1742-5468/acccdf.

Roche, A. A., Dole, P., & Bouzziri, M. (1994). Measurement of the practical adhesion of paint coatings to metallic sheets by the pull-off and three-point flexure tests. *Journal of Adhesion Science and Technology*, *8*(6), 587–609. https://doi.org/10.1163/156856194x00366.

Rudawska, A. (2019). Comparison of the adhesive joints' strength of the similar and dissimilar systems of metal alloy/polymer composite. *Applied Adhesion Science*, *7*(1), 7. https://doi.org/10.1186/s40563-019-0123-x.

Rybicki, E. F., & Kanninen, M. F. (1977). A finite element calculation of stress intensity factors by a modified crack closure integral. *Engineering Fracture Mechanics*, *9*(4), 931–938. https://doi.org/10.1016/0013-7944(77)90013-3.

Saeb, S., Firooz, S., Steinmann, P., & Javili, A. (2021). Generalized interfaces via weighted averages for application to graded interphases at large deformations. *Journal of the Mechanics and Physics of Solids*, *149*, 104234. https://doi.org/10.1016/j.jmps.2020.104234.

Saikia, P. J., & Muthu, N. (2024). Estimation of CZM parameters for investigating the interface fracture of adhesively bonded joints under mode I, mode II, and mixed-mode (I/II) loading. *Fatigue and Fracture of Engineering Materials and Structures*, *47*(12), 4636–4649. https://doi.org/10.1111/ffe.14457.

Santos, J. P. J. R., Correia, D. S., Marques, E. A. S., Carbas, R. J. C., Gilbert, F., & Silva, L. F. M., da (2023). Extended finite element method (XFEM) model for the damage mechanisms present in joints bonded using adhesives doped with inorganic fillers. *Materials*, *16*(23), 7499. https://doi.org/10.3390/ma16237499.

Savitzky, A., & Golay, M. J. E. (1964). Smoothing and differentiation of data by simplified least squares procedures. *Analytical Chemistry*, *36*(8), 1627–1639. https://doi.org/10.1021/ac60214a047.

Scattina, A., Peroni, L., Peroni, M., & Avalle, M. (2011). Numerical analysis of hybrid joining in car body applications. *Journal of Adhesion Science and Technology*, *25*(18), 2409–2433. https://doi.org/10.1163/016942411X580117.

Schaller, E., Javili, A., Schmidt, I., Papastavrou, A., & Steinmann, P. (2022). A peridynamic formulation for nonlocal bone remodelling. *Computer Methods in Biomechanics and Biomedical Engineering*, *25*(16), 1835–1851. https://doi.org/10.1080/10255842.2022.2039641.

Schmandt, Ch., & Marzi, S. (2025). A strain-rate-dependent cohesive zone model for peel-loaded thick and flexible adhesive layers of various geometries prone to stick-slip failure. *Theoretical and Applied Fracture Mechanics*, *136*, 104755. https://doi.org/10.1016/j.tafmec.2024.104755.

Schmelzle, L., Striewe, M., Mergheim, J., Meschut, G., Possart, G., Teutenberg, D., Hein, D., & Steinmann, P. (2023). Testing, modelling, and parameter identification for adhesively bonded joints under the influence of temperature. *Journal of Adhesion Science and Technology*, *37*(16), 2285–2316. https://doi.org/10.1080/01694243.2022.2125714.

Senthil, K., Arockiarajan, A., & Palaninathan, R. (2018). Numerical study on the onset of initiation of debond growth in adhesively bonded composite joints. *International Journal of Adhesion and Adhesives*, *84*, 202–219. https://doi.org/10.1016/j.ijadhadh.2018.03.009.

Shell, M. S. (2016). Coarse-graining with the relative entropy. In S. A. Rice, A. R. Dinner (Eds.), *Advances in Chemical Physics* (vol. 161, pp. 395–441). John Wiley & Sons. https://doi.org/10.1002/9781119290971.ch5.

Shi, T., & Zhang, Y. (2024). A length-free phase field model for epoxy adhesive materials based on modified Drucker–Prager criterion. *Composite Structures*, *346*, 118450. https://doi.org/10.1016/j.compstruct.2024.118450.

Shi, T., Livi, S., Duchet-Rumeau, J., & Gérard, J.-F. (2021). Enhanced mechanical and thermal properties of ionic liquid core/silica shell microcapsules-filled epoxy microcomposites. *Polymer*, *233*, 124182. https://doi.org/10.1016/j.polymer.2021.124182.

Shim, M.-J., & Kim, S.-W. (1997). Cure reaction and mechanical properties of DGEBA/MDA/nitrile system. *Materials Chemistry and Physics*, *47*(2–3), 198–202. https://doi.org/10.1016/S0254-0584(97)80051-X.

Shin, K. Ch., & Lee, J. J. (2003). Bond parameters to improve tensile load bearing capacities of co-cured single and double lap joints with steel and carbon fiber-epoxy composite adherends. *Journal of Composite Materials*, *37*(5), 401–420. https://doi.org/10.1177/0021998303037005040.

Shishesaz, M., & Hosseini, M. (2018). Effects of joint geometry and material on stress distribution, strength and failure of bonded composite joints: An overview. *The Journal of Adhesion*, *96*(12), 1053–1121. https://doi.org/10.1080/00218464.2018.1554483.

Shokuhfar, A., & Arab, B. (2013). The effect of cross linking density on the mechanical properties and structure of the epoxy polymers: Molecular dynamics simulation. *Journal of Molecular Modeling*, *19*(9), 3719–3731. https://doi.org/10.1007/s00894-013-1906-9.

Silling, S. A. (2000). Reformulation of elasticity theory for discontinuities and long-range forces. *Journal of the Mechanics and Physics of Solids*, *48*(1), 175–209. https://doi.org/10.1016/s0022-5096(99)00029-0.

Silling, S. A., Epton, M., Weckner, O., Xu, J., & Askari, E. (2007). Peridynamic states and constitutive modeling. *Journal of Elasticity*, *88*(2), 151–184. https://doi.org/10.1007/s10659-007-9125-1.

Silva, L. F. M., da, & Campilho, R. D. S. G. (2011). *Advances in Numerical Modeling of Adhesive Joints*. Springer Berlin, Heidelberg. https://doi.org/10.1007/978-3-642-23608-2.

Silva, L. F. M., da, Rodrigues, T. N. S. S., Figueiredo, M. A. V., Moura, M. F. S. F., de, & Chousal, J. A. G. (2006). Effect of adhesive type and thickness on the lap shear strength. *The Journal of Adhesion*, *82*(11), 1091–1115. https://doi.org/10.1080/00218460600948511.

Silva, L. F. M., da, Neves, P. J., das, Adams, R., & Spelt, J. (2009a). Analytical models of adhesively bonded joints – Part I: Literature survey. *International Journal of Adhesion and Adhesives*, *29*(3), 319–330. https://doi.org/10.1016/j.ijadhadh.2008.06.005.

Silva, L. F. M., da, Neves, P. J., das, Adams, R., Wang, A., & Spelt, J. (2009b). Analytical models of adhesively bonded joints – Part II: Comparative study. *International Journal of Adhesion and Adhesives*, *29*(3), 331–341. https://doi.org/10.1016/j.ijadhadh.2008.06.007.

Sluis, O., van der, Iwamoto, N., Qu, J., Yang, S., Yuan, C., Driel, W. D., van, & Zhang, G. Q. (2018). Advances in delamination modeling of metal/polymer systems: Atomistic aspects. In J. E. Morris (Ed.), *Nanopackaging: Nanotechnologies and Electronics Packaging* (pp. 129–183). Springer Cham.

Smit, R. J. M., Brekelmans, W. A. M., & Meijer, H. E. H. (1998). Prediction of the mechanical behavior of nonlinear heterogeneous systems by multi-level finite element modeling. *Computer Methods in Applied Mechanics and Engineering*, *155*(1–2), 181–192. https://doi.org/10.1016/S0045-7825(97)00139-4.

Solar, M., Qin, Z., & Buehler, M. J. (2014). Molecular mechanics and performance of crosslinked amorphous polymer adhesives. *Journal of Materials Research*, *29*(9), 1077–1085. https://doi.org/10.1557/jmr.2014.82.

Soliman, S. M. A., Abdelhakim, M., & Sabaa, M. W. (2024). Study curing of epoxy resin by Isophoronediamine/Triethylenetetramine and reinforced with montmorillonite and effect on compressive strength. *BMC Chemistry*, *18*(1), 211. https://doi.org/10.1186/s13065-024-01319-8.

Soutis, C. (2005). Carbon fiber reinforced plastics in aircraft construction. *Materials Science and Engineering: A*, *412*(1–2), 171–176. https://doi.org/10.1016/j.msea.2005.08.064.

Spannraft, L., Possart, G., Steinmann, P., & Mergheim, J. (2022). Generalized interfaces enabling macroscopic modeling of structural adhesives and their failure. *Forces in Mechanics*, *9*, 100137. https://doi.org/10.1016/j.finmec.2022.100137.

Spannraft, L., Steinmann, P., & Mergheim, J. (2023). A generalized anisotropic damage interface model for finite strains. *Journal of the Mechanics and Physics of Solids*, *174*, 105255. https://doi.org/10.1016/j.jmps.2023.105255.

Steinmann, P., & Runesson, K. (2021). *The Catalogue of Computational Material Models: Basic Geometrically Linear Models in 1D*. Springer Cham. https://doi.org/10.1007/978-3-030-63684-5.

Stevens, M. J. (2001). Interfacial fracture between highly cross-linked polymer networks and a solid surface: Effect of interfacial bond density. *Macromolecules*, *34*(8), 2710–2718. https://doi.org/10.1021/ma000553u.

Stewart, I., Chambers, A., & Gordon, T. (2007). The cohesive mechanical properties of a toughened epoxy adhesive as a function of cure level. *International Journal of Adhesion and Adhesives*, *27*(4), 277–287. https://doi.org/10.1016/j.ijadhadh.2006.05.003.

Subramaniyan, A. K., & Sun, C. T. (2008). Continuum interpretation of virial stress in molecular simulations. *International Journal of Solids and Structures*, *45*(14–15), 4340–4346. https://doi.org/10.1016/j.ijsolstr.2008.03.016.

Sugiman, S., Crocombe, A. D., & Aschroft, I. A. (2013). Experimental and numerical investigation of the static response of environmentally aged adhesively bonded joints. *International Journal of Adhesion and Adhesives*, *40*, 224–237. https://doi.org/10.1016/j.ijadhadh.2012.08.007.

Sun, H. (1998). COMPASS: An ab initio force-field optimized for condensed-phase applications overview with details on alkane and benzene compounds. *The Journal of Physical Chemistry B*, *102*(38), 7338–7364. https://doi.org/10.1021/jp980939v.

Sundararaghavan, V., & Kumar, A. (2013). Molecular dynamics simulations of compressive yielding in cross-linked epoxies in the context of argon theory. *International Journal of Plasticity*, *47*, 111–125. https://doi.org/10.1016/j.ijplas.2013.01.004.

Tadmor, E. B., & Miller, R. E. (2011). *Modeling Materials: Continuum, Atomistic and Multiscale Techniques*. Cambridge University Press. https://doi.org/10.1017/CBO9781139003582.

Tadmor, E. B., Ortiz, M., & Phillips, R. (1996). Quasicontinuum analysis of defects in solids. *Philosophical Magazine A*, *73*(6), 1529–1563. https://doi.org/10.1080/01418619608243000.

Tadmor, E. B., Miller, R. E., & Elliott, R. S. (2012). *Continuum Mechanics and Thermodynamics: From Fundamental Concepts to Governing Equations*. Cambridge University Press.

Taib, A. A., Boukhili, R., Achiou, S., Gordon, S., & Boukehili, H. (2006). Bonded joints with composite adherends. Part I. Effect of specimen configuration, adhesive thickness, spew fillet and adherend stiffness on fracture. *International Journal of Adhesion and Adhesives*, *26*(4), 226–236. https://doi.org/10.1016/j.ijadhadh.2005.03.015.

Tam, L.-h., & Lau, D. (2014). A molecular dynamics investigation on the cross-linking and physical properties of epoxy-based materials. *RSC Advances*, *4*(62), 33074–33081. https://doi.org/10.1039/C4RA04298K.

Tam, L.-h., & Lau, D. (2015). Moisture effect on the mechanical and interfacial properties of epoxy-bonded material system: An atomistic and experimental investigation. *Polymer*, *57*, 132–142. https://doi.org/10.1016/j.polymer.2014.12.026.

Tam, L.-h., & Lau, D. (2016). Effect of structural voids on mesoscale mechanics of epoxy-based materials. *Coupled Systems Mechanics*, *5*(4), 355–369. https://doi.org/10.12989/csm.2016.5.4.355.

Tavares, M. I. B., D'almeida, J. R. M., & Monteiro, S. N. (2000). ^{13}C solid-state NMR analysis of the DGEBA/TETA epoxy system. *Journal of Applied Polymer Science*, *78*(13), 2358–2362. https://doi.org/10.1002/1097-4628(20001220)78:13%3C2358::AID-APP120%3E3.0.CO;2-T.

Theodorou, D. N., & Suter, U. W. (1986). Atomistic modeling of mechanical properties of polymeric glasses. *Macromolecules*, *19*(1), 139–154. https://doi.org/10.1021/ma00155a022.

Thompson, A. P., Plimpton, S. J., & Mattson, W. (2009). General formulation of pressure and stress tensor for arbitrary many-body interaction potentials under periodic boundary conditions. *The Journal of Chemical Physics*, *131*(15), 154107. https://doi.org/10.1063/1.3245303.

Thompson, A. P., Aktulga, H. M., Berger, R., Bolintineanu, D. S., Brown, W. M., Crozier, P. S., Veld, P. J., in't, Kohlmeyer, A., Moore, S. G., Nguyen, T. D., Shan, R., Stevens, M. J., Tranchida, J., Trott, Ch., & Plimpton, S. J. (2022). LAMMPS – a flexible simulation tool for particle-based materials modeling at the atomic, meso, and continuum scales. *Computer Physics Communications*, *271*, 108171. https://doi.org/10.1016/j.cpc.2021.108171.

Tkachuk, A. I., Zagora, A. G., Terekhov, I. V., & Mukhametov, R. R. (2022). Isophorone diamine – a curing agent for epoxy resins: Production, application, prospects. A review. *Polymer Science, Series D*, *15*(2), 171–176. https://doi.org/10.1134/S1995421222020289.

Treloar, L. R. G. (1975). *The Physics of Rubber Elasticity* (3rd ed.). Clarendon Press.

Tserpes, K., Barroso-Caro, A., Carraro, P. A., Beber, V. C., Floros, I., Gamon, W., Kozłowski, M., Santandrea, F., Shahverdi, M., Skejić, D., Bedon, Ch., & Rajčić, V. (2021). A review on failure theories and simulation models for adhesive joints. *The Journal of Adhesion*, *98*(12), 1855–1915. https://doi.org/10.1080/00218464.2021.1941903.

Vakhrushev, A. V. (2018). Introductory chapter: Molecular dynamics: Basic tool of nanotechnology simulations for "Production 4.0" revolution. In A. V. Vakhrushev (Ed.), *Molecular Dynamics*. InTech. https://doi.org/10.5772/intechopen.79045.

Vallée, T., Correia, J. R., & Keller, T. (2006). Probabilistic strength prediction for double lap joints composed of pultruded GFRP profiles part I: Experimental and numerical investigations. *Composites Science and Technology*, *66*(13), 1903–1914. https://doi.org/10.1016/j.compscitech.2006.04.007.

Varshney, V., Patnaik, S. S., Roy, A. K., & Farmer, B. L. (2008). A molecular dynamics study of epoxy-based networks: Cross-linking procedure and prediction of molecular and material properties. *Macromolecules*, *41*(18), 6837–6842. https://doi.org/10.1021/ma801153e.

Verlet, L. (1967). Computer "experiments" on classical fluids. I. Thermodynamical properties of Lennard–Jones molecules. *Physical Review*, *159*(1), 98–103. https://doi.org/10.1103/physrev.159.98.

Viana, G., Machado, J., Carbas, R., Costa, M., Silva, L. M. F., da, Vaz, M., & Banea, M. D. (2018). Strain rate dependence of adhesive joints for the automotive industry at low and high temperatures. *Journal of Adhesion Science and Technology*, *32*(19), 2162–2179. https://doi.org/10.1080/01694243.2018.1464635.

Vu-Bac, N., Bessa, M. A., Rabczuk, T., & Liu, W. K. (2015). A multiscale model for the quasi-static thermo-plastic behavior of highly cross-linked glassy polymers. *Macromolecules*, *48*(18), 6713–6723. https://doi.org/10.1021/acs.macromol.5b01236.

Wang, Ch., Li, Y., Tao, L., Li, Y., Hu, L., & Feng, Z. (2025). Isogeometric analysis of adhesion between visco-hyperelastic material based on modified exponential cohesive zone model. *Computer Methods in Applied Mechanics and Engineering*, *434*, 117562. https://doi.org/10.1016/j.cma.2024.117562.

Wang, H.-T., & Wu, G. (2018). Bond-slip models for CFRP plates externally bonded to steel substrates. *Composite Structures*, *184*, 1204–1214. https://doi.org/10.1016/j.compstruct.2017.10.033.

Wang, J., Wolf, R. M., Caldwell, J. W., Kollman, P. A., & Case, D. A. (2004). Development and testing of a general amber force field. *Journal of Computational Chemistry*, *25*(9), 1157–1174. https://doi.org/10.1002/jcc.20035.

Ward, I. M., & Sweeney, J. (2012). *Mechanical Properties of Solid Polymers* (3rd ed.). John Wiley & Sons.

Weber, F., Ries, M., Bauer, Ch., Wick, Ch. R., & Pfaller, S. (2023). On equilibrating non-periodic molecular dynamics samples for coupled particle-continuum simulations of amorphous polymers. *Forces in Mechanics*, *10*, 100159. https://doi.org/10.1016/j.finmec.2022.100159.

Weber, F., Dötschel, V., Steinmann, P., Pfaller, S., & Ries, M. (2024). Evaluating the impact of filler size and filler content on the stiffness, strength, and toughness of polymer nanocomposites using coarse-grained molecular dynamics. *Engineering Fracture Mechanics*, *307*, 110270. https://doi.org/10.1016/j.engfracmech.2024.110270.

Weber, F., Vassaux, M., Laubert, L., & Pfaller, S. (2025). *How to properly measure the fracture properties of brittle materials using molecular simulations? Application to mode I and mode III in silica glass*. arXiv. https://doi.org/10.48550/arXiv.2501.16537.

Wehlack, C., & Possart, W. (2005). Chapter 6. Chemical structure formation and morphology in ultrathin polyurethane films on metals. In W. Possart (Ed.), *Adhesion: Current Research and Applications* (pp. 71–88). Wiley-VCH. https://doi.org/10.1002/3527607307.ch6.

Wei, Y., Jin, X., Luo, Q., Li, Q., & Sun, G. (2024). Adhesively bonded joints – a review on design, manufacturing, experiments, modeling and challenges. *Composites Part B: Engineering*, *276*, 111225. https://doi.org/10.1016/j.compositesb.2024.111225.

Weiner, S. J., Kollman, P. A., Nguyen, D. T., & Case, D. A. (1986). An all atom force field for simulations of proteins and nucleic acids. *Journal of Computational Chemistry*, *7*(2), 230–252. https://doi.org/10.1002/jcc.540070216.

White, S. R., Mather, P. T., & Smith, M. J. (2002). Characterization of the cure-state of DGEBA-DDS epoxy using ultrasonic, dynamic mechanical, and thermal probes. *Polymer Engineering & Science*, *42*(1), 51–67. https://doi.org/10.1002/pen.10927.

Wu, Ch., & Xu, W. (2006). Atomistic molecular modelling of crosslinked epoxy resin. *Polymer*, *47*(16), 6004–6009. https://doi.org/10.1016/j.polymer.2006.06.025.

Wu, Ch., & Xu, W. (2007). Atomistic molecular simulations of structure and dynamics of crosslinked epoxy resin. *Polymer*, *48*(19), 5802–5812. https://doi.org/10.1016/j.polymer.2007.07.019.

Wu, Y., Liu, J., Liu, H., Zhang, Z., Chen, P., & Huang, X. (2025). Mechanical analysis of bone fracture treatment with hydrogel adhesives. *International Journal of Adhesion and Adhesives*, *136*, 103873. https://doi.org/10.1016/j.ijadhadh.2024.103873.

Xia, W., Song, J., Jeong, C., Hsu, D. D., Phelan Jr., F. R., Douglas, J. F., & Keten, S. (2017). Energy-renormalization for achieving temperature transferable coarse-graining of polymer dynamics. *Macromolecules*, *50*(21), 8787–8796. https://doi.org/10.1021/acs.macromol.7b01717.

Xia, W., Hansoge, N. K., Xu, W.-S., Phelan Jr., F. R., Keten, S., & Douglas, J. F. (2019). Energy renormalization for coarse-graining polymers having different segmental structures. *Science Advances*, *5*(4). https://doi.org/10.1126/sciadv.aav4683.

Xia, W., Oterkus, E., & Oterkus, S. (2021). Ordinary state-based peridynamic homogenization of periodic micro-structured materials. *Theoretical and Applied Fracture Mechanics*, *113*, 102960. https://doi.org/10.1016/j.tafmec.2021.102960.

Xiao, G. Z., Delamar, M., & Shanahan, M. (1997). Irreversible interactions between water and dgeba/dda epoxy resin during hygrothermal aging. *Journal of Applied Polymer Science*, *65*(3), 449–458. https://doi.org/10.1002/(sici)1097-4628(19970718)65:3<449::aid-app4>3.0.co;2-h.

Xu, W., & Wei, Y. (2013). Influence of adhesive thickness on local interface fracture and overall strength of metallic adhesive bonding structures. *International Journal of Adhesion and Adhesives*, *40*, 158–167. https://doi.org/10.1016/j.ijadhadh.2012.07.012.

Yagyu, H., Hirai, Y., Uesugi, A., Makino, Y., Sugano, K., Tsuchiya, T., & Tabata, O. (2012). Simulation of mechanical properties of epoxy-based chemically amplified resist by coarse-grained molecular dynamics. *Polymer*, *53*(21), 4834–4842. https://doi.org/10.1016/j.polymer.2012.08.050.

Yang, S., & Qu, J. (2014a). An investigation of the tensile deformation and failure of an epoxy/Cu interface using coarse-grained molecular dynamics simulations. *Modelling and Simulation in Materials Science and Engineering*, *22*(6), 065011. https://doi.org/10.1088/0965-0393/22/6/065011.

Yang, S., & Qu, J. (2014b). Coarse-grained molecular dynamics simulations of the tensile behavior of a thermosetting polymer. *Physical Review E*, *90*(1), 012601. https://doi.org/10.1103/physreve.90.012601.

Yang, S., Gao, F., & Qu, J. (2013). A molecular dynamics study of tensile strength between a highly-crosslinked epoxy molding compound and a copper substrate. *Polymer*, *54*(18), 5064–5074. https://doi.org/10.1016/j.polymer.2013.07.019.

Yang, S., Cui, Z., & Qu, J. (2014). A coarse-grained model for epoxy molding compound. *The Journal of Physical Chemistry B*, *118*(6), 1660–1669. https://doi.org/10.1021/jp409297t.

Yarovsky, I., & Evans, E. (2002). Computer simulation of structure and properties of crosslinked polymers: Application to epoxy resins. *Polymer*, *43*(3), 963–969. https://doi.org/10.1016/S0032-3861(01)00634-6.

Yudhanto, A., Alfano, M., & Lubineau, G. (2021). Surface preparation strategies in secondary bonded thermoset-based composite materials: A review. *Composites Part A: Applied Science and Manufacturing*, *147*, 106443. https://doi.org/10.1016/j.compositesa.2021.106443.

Zernsdorf, K., Mechtcherine, V., Curbach, M., & Bösche, T. (2024). Numerical material testing of mineral-impregnated carbon fiber reinforcement for concrete. *Materials*, *17*(3), 737. https://doi.org/10.3390/ma17030737.

Zhang, S., Yu, T., & Chen, G. (2017). Reinforced concrete beams strengthened in flexure with near-surface mounted (NSM) CFRP strips: Current status and research needs. *Composites Part B: Engineering*, *131*, 30–42. https://doi.org/10.1016/j.compositesb.2017.07.072.

Zhao, W., Steinmann, P., & Pfaller, S. (2021). A particle-continuum coupling method for multiscale simulations of viscoelastic–viscoplastic amorphous glassy polymers. *International Journal for Numerical Methods in Engineering*, *122*(24), 7431–7451. https://doi.org/10.1002/nme.6836.

Zhou, M. (2003). A new look at the atomic level virial stress: On continuum-molecular system equivalence. *Proceedings of the Royal Society A: Mathematical, Physical and Engineering Sciences*, *459*(2037), 2347–2392. https://doi.org/10.1098/rspa.2003.1127.

Zienkiewicz, O. C., Taylor, R. L., & Zhu, J. Z. (2005). *The Finite Element Method Set*. Elsevier.

Zimmerman, J. A., Webb III, E. B., Hoyt, J. J., Jones, R. E., Klein, P. A., & Bammann, D. J. (2004). Calculation of stress in atomistic simulation. *Modelling and Simulation in Materials Science and Engineering*, *12*(4), S319. https://www.doi.org/10.1088/0965-0393/12/4/S03.

Appendix A

List of abbreviations

CFRP	carbon-fiber reinforced polymer
CGMD	coarse-grained molecular dynamics
COH	formyl group
COOH	carboxyl group
CPD	continuum-kinematics-inspired peridynamics
CZM	cohesive zone model
DCB	double cantilever beam
DDS	4,4'-diaminodiphenylsulfone
DETA	diethylenetriamine
DETDA	diethyltoluene diamine
DGEBA	diglycidyl ether of bisphenol A
DLJ	double-lap joint
DPD	dissipative particle dynamics
EDX	energy-dispersive X-ray microanalysis
ENF	end-notched flexure
FEM	finite element method
FRP	fiber-reinforced polymer
GFRP	glass-fiber-reinforced polymer
GIM	generalized interface models
IBI	iterative Boltzmann inversion
IPD	isophorone diamine
LaSAT	laser shock adhesion test
MD	molecular dynamics
MDA	4,4'-methylenedianiline
MMB	mixed-mode bending
MS-CG	multiscale coarse-graining method
NH2	amine group
NPT	isothermal-isobaric ensemble
NVE	micro-canonical ensemble
NVT	canonical ensemble
OH	hydroxyl group
PACM	4,4-diaminodicyclohexylmethane
PD	peridynamics
PFM	phase-field fracture model
PMF	potential of mean force
PR	Parinello–Rahman
SLJ	single-lap joint
SMD	steered molecular dynamics
TAPO	toughened adhesive polymer
TETA	triethylenetetramine
TSL	traction-separation law
VCCT	virtual crack closure technique
XFEM	extended finite element method